Figure S2. Generation of Cardiac-specific ATRAP Transgenic Mice

(**A**) Transgenic mice expressing ATRAP specifically in cardiomyocytes were generated on a C57BL/6J background with standard techniques. Briefly, a 5.5-kb fragment of the mouse a-myosin heavy chain (MHC) promoter (a kind gift from Dr. Jeffrey Robbins, University of Cincinnati, Cincinnati, OH) [1] and a mouse ATRAP cDNA [2,3] were subcloned into a pBsKs(-) plasmid. The resultant recombinant plasmid, pMHC-ATRAP, was digested with *Kpn*I and *Not*I to generate a ~6.3 kb of DNA fragment consisting of the ? -MHC promoter, mouse ATRAP cDNA, and the bovine growth hormone polyadenylation sequence (BGH polyA). This construct was microinjected into the pronucleus of fertilized mouse embryos. The resulting pups were screened for the presence of the transgene by PCR, using forward (TGCTTGGGGCAACTTCACTATC) and reverse (ACGGTGCATGTGGTAGACGAG) primers. F and R indicate the locations of the forward and reverse primers used for genotyping by PCR, respectively. (**B**) Quantitative analysis of ATRAP expression at the protein level revealed the highest and moderate expression levels of ATRAP in lines 52 and 46 (Tg52 and Tg46), respectively, among the 10 obtained lines of transgenic mice and these two lines of transgenic mice were further characterized. (**C**) To examine the transgene copy number in the transgenic mice, Tg46 and Tg52, genomic DNA was isolated from kidneys of littermate control mice and these transgenic mice, digested by *Dra*I, and subjected to Southern blot analysis. The results of Southern blot analysis showed that Tg46 had one copy and Tg52 had nine copies of the transgene. (**D**) The results of real-time quantitative RT-PCR analysis showed 59- and 244-fold increases in cardiac ATRAP mRNA expression over littermate control mice in Tg46 and Tg52, respectively. (**E**) The results of Western blot analysis also showed unaltered extracardiac ATRAP expression in Tg46 and Tg52 mice.

Fig. S3

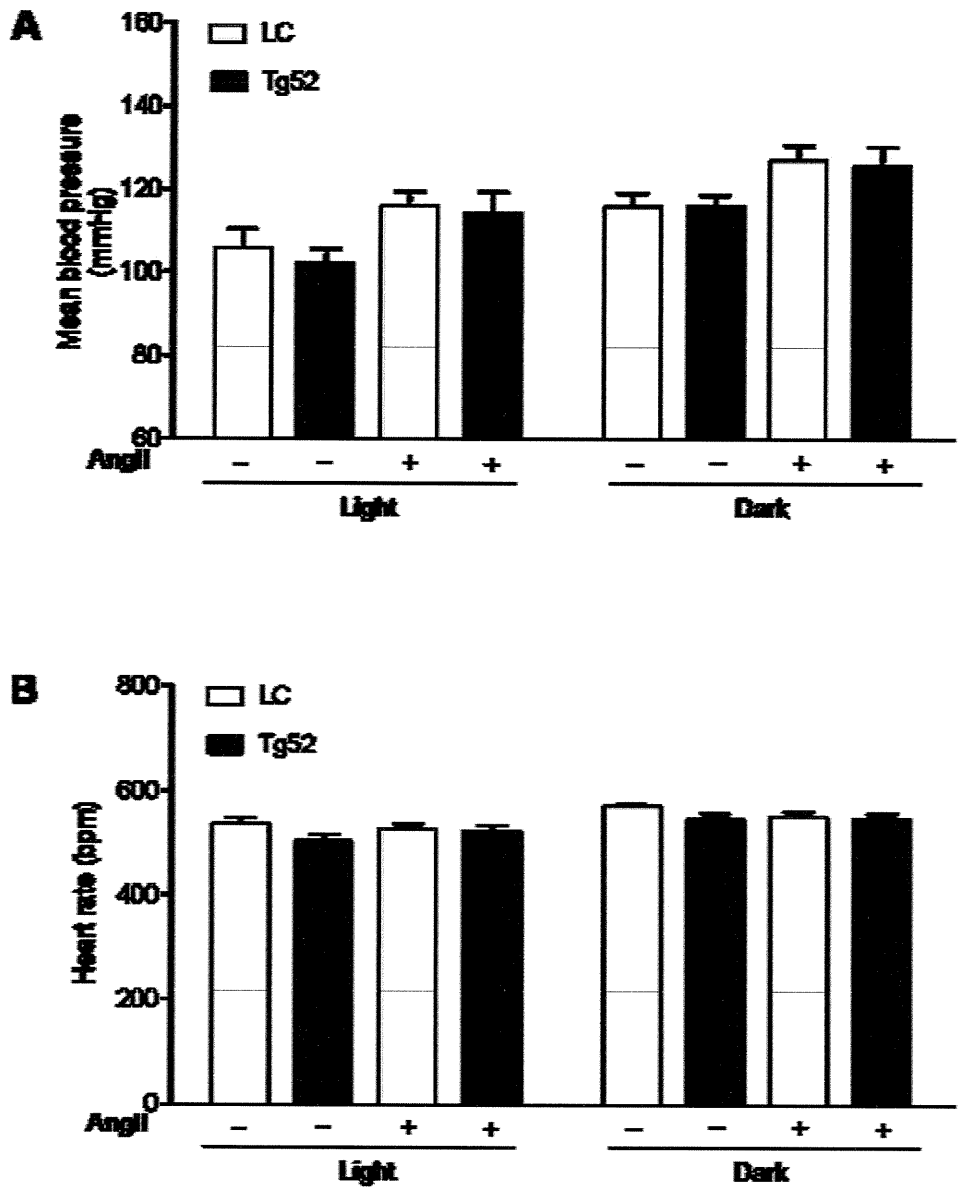

Figure S3. Direct Mean BP and HR measurement by radiotelemetric devices in LC and Tg mice

(**A**) In LC mice, Ang II infusion for 2 weeks tended to increase the mean BP (MBP) in the light period (105.7±4.6 versus 116.0±3.5 mmHg, *P*=0.126) and in the dark period (115.8±3.4 versus 126.9±3.8 mmHg, *P*=0.076), without statistical significance. Similarly in Tg52 mice, Ang II infusion tended to increase MBP in the light period (102.4±3.3 versus 114.3±5.0 mmHg, *P*=0.071) and in the dark period (115.9±2.8 versus 125.7±4.6 mmHg, *P*=0.126), also without statistical significance. (**B**) Regarding the radiotelemetric heart rate (HR), Ang II in fusion did not affect HR in LC and Tg mice in either the light period or the dark period.

Am J Physiol Renal Physiol 299: F991–F1003, 2010.
First published August 25, 2010; doi:10.1152/ajprenal.00738.2009.

Intrarenal suppression of angiotensin II type 1 receptor binding molecule in angiotensin II-infused mice

Hiromichi Wakui,[1]* Kouichi Tamura,[1]* Miyuki Matsuda,[1] Yunzhe Bai,[2] Toru Dejima,[1] Atsu-ichiro Shigenaga,[1] Shin-ichiro Masuda,[1] Koichi Azuma,[1] Akinobu Maeda,[1] Tomonori Hirose,[3] Tomoaki Ishigami,[1] Yoshiyuki Toya,[1] Machiko Yabana,[1] Susumu Minamisawa,[4] and Satoshi Umemura[1]

[1]*Department of Medical Science and Cardiorenal Medicine,* [2]*Cardiovascular Research Institute, and* [3]*Department of Molecular Biology, Yokohama City University Graduate School of Medicine, Yokohama; and* [4]*Department of Life Science and Medical Bio-science, Waseda University, Tokyo, Japan*

Submitted 28 December 2009; accepted in final form 23 August 2010

Wakui H, Tamura K, Matsuda M, Bai Y, Dejima T, Shigenaga A, Masuda S, Azuma K, Maeda A, Hirose T, Ishigami T, Toya Y, Yabana M, Minamisawa S, Umemura S. Intrarenal suppression of angiotensin II type 1 receptor binding molecule in angiotensin II-infused mice. *Am J Physiol Renal Physiol* 299: F991–F1003, 2010. First published August 25, 2010; doi:10.1152/ajprenal.00738.2009.—ATRAP [ANG II type 1 receptor (AT1R)-associated protein] is a molecule which directly interacts with AT1R and inhibits AT1R signaling. The aim of this study was to examine the effects of continuous ANG II infusion on the intrarenal expression and distribution of ATRAP and to determine the role of AT1R signaling in mediating these effects. C57BL/6 male mice were subjected to vehicle or ANG II infusions at doses of 200, 1,000, or 2,500 ng·kg^{-1}·min^{-1} for 14 days. ANG II infusion caused significant suppression of ATRAP expression in the kidney but did not affect ATRAP expression in the testis or liver. Although only the highest ANG II dose (2,500 ng·kg^{-1}·min^{-1}) provoked renal pathological responses, such as an increase in the mRNA expression of angiotensinogen and the α-subunit of the epithelial sodium channel, ANG II-induced decreases in ATRAP were observed even at the lowest dose (200 ng·kg^{-1}·min^{-1}), particularly in the outer medulla of the kidney, based on immunohistochemical staining and Western blot analysis. The decrease in renal ATRAP expression by ANG II infusion was prevented by treatment with the AT1R-specific blocker olmesartan. In addition, the ANG II-mediated decrease in renal ATRAP expression through AT1R signaling occurred without an ANG II-induced decrease in plasma membrane AT1R expression in the kidney. On the other hand, a transgenic model increase in renal ATRAP expression beyond baseline was accompanied by a constitutive reduction of renal plasma membrane AT1R expression and by the promotion of renal AT1R internalization as well as the decreased induction of angiotensinogen gene expression in response to ANG II. These results suggest that the plasma membrane AT1R level in the kidney is modulated by intrarenal ATRAP expression under physiological and pathophysiological conditions in vivo.

gene expression; renin-angiotensin system; angiotensin; receptor; hypertension

EVIDENCE SUGGESTS THAT THE activation of angiotensin II (ANG II) type 1 receptor (AT1R) through the tissue renin-angiotensin system plays a pivotal role in the pathogenesis and associated end-organ injury of hypertension. The carboxyl-terminal portion of AT1R is involved in the control of AT1R internalization independent of G protein coupling and plays an important role in linking receptor-mediated signal transduction to the specific pathophysiological response to ANG II (16, 41). The AT1R-associated protein (ATRAP), which is a molecule specifically interacting with the carboxyl-terminal domain of the AT1R, was cloned using a yeast-two-hybrid screening system (8, 21). The results of previous in vitro studies and ATRAP transgenic mice studies showed that ATRAP suppresses ANG II-mediated pathological responses in cardiovascular cells and tissues by promoting the constitutive internalization of AT1R (1, 7, 11, 30, 40, 44), thereby suggesting ATRAP to be an endogenous inhibitor of AT1R signaling (22, 37).

With respect to the tissue distribution and regulation of ATRAP expression in vivo, ATRAP and AT1R are broadly expressed in many tissues, including the kidney, and there is a tissue-specific regulatory balancing of the expression of ATRAP and AT1R during the development of hypertension in spontaneously hypertensive rats (35). Chronic infusion of ANG II is one of the representative models of hypertension and end-organ damage and is associated with the activation of the intrarenal renin-angiotensin system, including upregulation of renal angiotensinogen through the AT1R pathway (10, 20, 49). Furthermore, previous studies using a series of kidney cross-transplant experiments also showed that the activation of intrarenal AT1R is required for the development of ANG II-dependent hypertension and the related end-organ damage (5, 6). Thus we hypothesized that the intrarenal distribution and regulation of endogenous ATRAP expression may also be involved in the pathophysiological responses to ANG II. Accordingly, studies were performed to examine the changes in intrarenal ATRAP expression during ANG II infusion in mice and to determine the role of AT1R in mediating these responses. Furthermore, we examined whether the plasma membrane AT1R level was influenced by the ANG II-mediated decrease in the renal ATRAP level and/or by an increase in the renal ATRAP level in a transgenic model, to analyze the relationship between ATRAP and AT1R expression in the kidney.

METHODS

Materials. ANG II was purchased from Sigma. The AT1R-specific blocker olmesartan (RNH6270) was kindly supplied by Daiichi-Sankyo Pharmaceuticals (Tokyo, Japan).

Animals and ANG II infusion. Adult male C57BL/6 mice (10–12 wk of age, Oriental Yeast Kogyo) were divided into three groups (n = 6–8 mice/group) for the subcutaneous infusion of vehicle or ANG II (either 200, 1,000, or 2,500 ng·kg^{-1}·min^{-1}) via an osmotic minipump (ALZA) for 14 days. The percentage of body weight increase (% BW increase) was calculated as follows: % BW increase = [(BW at *day 14*) − (BW at baseline) × 100]/(BW at baseline). In several of the experiments, vehicle or olmesartan (10 mg·kg^{-1}·day^{-1}) in the

* H. Wakui and K. Tamura contributed equally to this work.

Address for reprint requests and other correspondence: K. Tamura, Dept. of Medical Science and Cardiorenal Medicine, Yokohama City Univ. Graduate School of Medicine, 3-9 Fukuura, Kanazawa-ku, Yokohama 236-0004, Japan (e-mail: tamukou@med.yokohama-cu.ac.jp).

drinking water was administrated for the same period. The ANG II and olmesartan dosages were determined from previous reports (10, 18, 48). Following experimental treatment, the mice were anesthetized and the tissues were removed into liquid nitrogen or fixative. The Animal Studies Committee of Yokohama City University approved all the animal experimental protocols.

Blood pressure measurements. Systolic blood pressure and heart rate were measured by the tail-cuff method (BP monitor MK-2000; Muromachi Kikai), as described previously (34, 42). BP monitor MK-2000 made it possible to measure blood pressure without preheating the animals, thus allowing the avoidance of stressful conditions (17).

Analysis of total ATRAP and AT1R protein expression. The characterization and specificity of the anti-mouse ATRAP antibody and the anti-AT1R antibody (sc-1173, Santa Cruz Biotechnology) were described previously (42). Western blot analysis was performed to examine the total protein expression of ATRAP and AT1R as described (40, 42). Briefly, whole tissue extracts were used for SDS-PAGE, and transferred membranes (Millipore) were incubated with either *1*) an anti-ATRAP antibody or *2*) an anti-AT1R antibody and subjected to enhanced chemiluminescence (Amersham Biosciences). The images were analyzed quantitatively using a Fuji LAS3000 Image Analyzer (Fujifilm) for determination of the total ATRAP and AT1R protein levels. To measure the tissue expression ratio of ATRAP to AT1R, each ATRAP protein level was divided by the corresponding total AT1R protein level obtained by reprobing, and thus was derived from the same extract.

Real-time quantitative RT-PCR analysis. Total RNA was extracted from the kidney with ISOGEN (Nippon Gene, Tokyo, Japan), and cDNA was synthesized using the SuperScript III First-Strand System (Invitrogen). Real-time quantitative RT-PCR was performed by incubating the RT product with TaqMan Universal PCR Master Mix and a designed TaqMan probe (Applied Biosystems), essentially as described previously (34). RNA quantity was expressed relative to the 18S rRNA endogenous control.

Immunohistochemistry for ATRAP and AT1R expression. Immunohistochemistry was performed as described previously (14, 42). The kidneys were perfusion-fixed with 4% paraformaldehyde, subsequently embedded in paraffin, and cut into sections of 4-μm thickness. The sections were dewaxed and rehydrated. Antigen retrieval was performed by microwave heating. The sections were treated for 60 min with 10% normal goat serum in phosphate-buffered saline and blocked for endogenous biotin activity using an Avidin/Biotin Blocking kit (Vector Laboratories). For the study of ATRAP and AT1R, the sections were incubated at 4°C overnight with either *1*) an anti-ATRAP antibody diluted at 1:100 or *2*) anti-AT1R antibody diluted at 1:100, as described previously (42). The sections were incubated for 60 min with (a) biotinylated goat anti-rabbit IgG (Nichirei), blocked for endogenous peroxidase activity by incubation with 0.3% H_2O_2 for 20 min, treated for 30 min with streptavidin and biotinylated peroxidase (DAKO), and then exposed to diaminobenzidine. The sections were counterstained with hematoxylin, dehydrated, and mounted. Immunoreactivity was semiquantitatively evaluated in a blinded manner. Briefly, 20 microscopic fields/slide were selected at random for evaluation. Examination was performed using a microscope with ×200 magnification (Olympus) and an integrated digital camera system (Olympus). Image Pro-plus computer image analysis software (Media Cybernetics, Bethesda, MD) was used to analyze the brown stain pixel density and to quantify the protein levels, as described previously (10, 15, 32, 47).

Analysis of plasma membrane AT1R expression. The plasma membrane was specifically extracted from tissues using a Plasma Membrane Extraction Kit (K268–50, Biovision) according to the manufacturer's protocol and then used for SDS-PAGE (43). Membranes (Millipore) were incubated with either *1*) anti-AT1R antibody or *2*) anti-flotillin-2 monoclonal antibody (no. 3436, Cell Signaling Technology) and subjected to enhanced chemiluminescence (Amersham Biosciences). Flotillin-2 is constitutively localized to the plasma membrane and was used as an internal control protein on the plasma membrane (36). The images were analyzed quantitatively using a Fuji LAS3000 Image Analyzer (Fujifilm) for determination of the plasma membrane AT1R protein levels.

Generation of ATRAP transgenic mice. To produce ATRAP transgenic mice, hemagglutinin (HA)-tagged mouse ATRAP cDNA was subcloned into pCAGGS expression vector, which contained a cytomegalovirus enhancer and chicken β-actin (CAG) promoter (28), and the resultant transgene construct was microinjected into the pronuclei of fertilized mouse embryos at the single-cell stage to generate transgenic mice (C57BL/6 strain). The ATRAP transgene positive (+) mice were mated with C57BL/6 wild-type mice to obtain ATRAP transgene positive (+) mice and littermate control mice for the experiments. Animal genotyping was performed as previously described. Transgenic mice were identified by PCR using 5′-TGCTT-

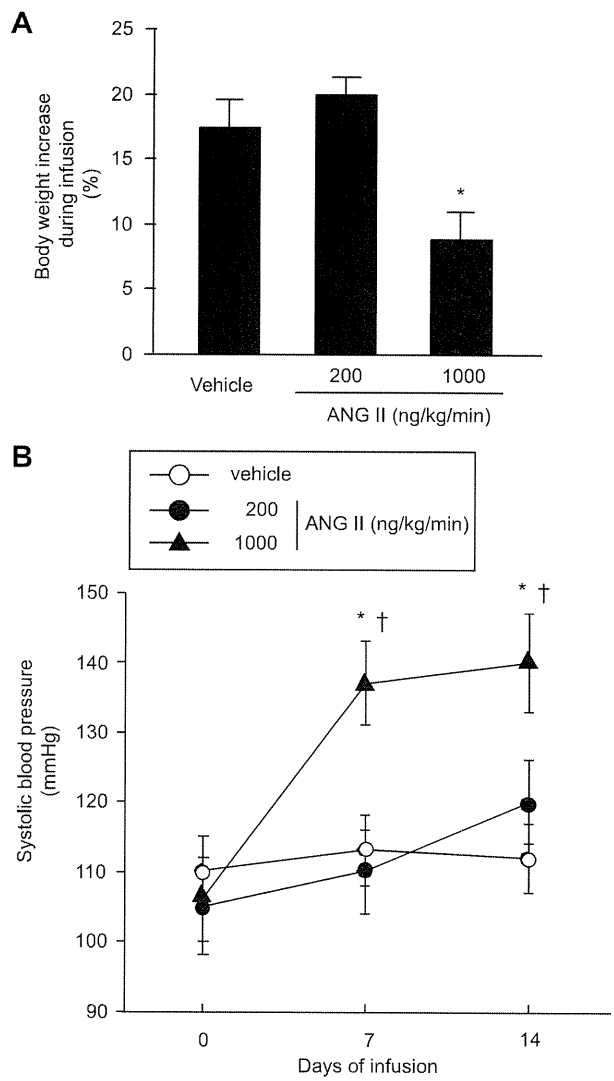

Fig. 1. Effects of continuous ANG II infusion on body weight (*A*) and systolic blood pressure (*B*) during the treatment period. Adult male C57BL/6 mice were divided into 3 groups (n = 6–8 mice/group) for the subcutaneous infusion of vehicle or ANG II (either 200 or 1,000 ng·kg^{-1}·min^{-1}) via an osmotic minipump for 14 days. The values of the percent body weight increase and systolic blood pressure are expressed as means ± SE (n = 6–8/group). *P < 0.05 vs. vehicle. †P < 0.05 vs. *day 0*.

GGGGCAACTTCACTATC-3′ as the forward primer and 5′-ACGGTGCATGTGGTAGACGAG-3′ as the reverse primer.

Statistical analysis. Values are expressed as means ± SE in the text and figures. The data were analyzed using ANOVA. If a statistically significant effect was found, a post hoc analysis with Scheffé's test was performed to detect differences between the groups. Values of $P < 0.05$ were considered statistically significant.

RESULTS

Effects of ANG II on body weight and systolic blood pressure. Vehicle-infused mice gained BW during the study period (%BW increase, 17.2 ± 2.2%, $n = 8$) (Fig. 1*A*). Mice infused at a low dose of ANG II (200 ng·kg^{-1}·min^{-1}) displayed a similar gain in BW (%BW increase, 19.9 ± 1.4%, $n = 6$). In contrast, mice subjected to a high dose of ANG II (1,000 ng·kg^{-1}·min^{-1}) exhibited a significant inhibition of BW gain (%BW increase, 8.7 ± 2.1%, $n = 7$, $P < 0.05$ vs. vehicle and $P < 0.01$ vs. ANG II 200 ng·kg^{-1}·min^{-1}). All groups displayed the same range of systolic blood pressure, as determined by tail-cuff plethysmography (105–110 mmHg) at baseline (Fig. 1*B*). Systolic blood pressure remained stable in the vehicle-infused mice during the study period, with systolic blood pressure averaging 113 ± 6 and 112 ± 6 mmHg by *days 7* and *14*, respectively ($n = 8$). Similarly, systolic blood pressure did not exhibit any evident change in the low-dose ANG II (200 ng·kg^{-1}·min^{-1})-infused mice (110 ± 5 and 120 ± 5 mmHg by *days 7* and *14*, respectively, $n = 6$). In contrast, systolic blood pressure was significantly elevated, to 137 ± 6 and 140 ± 7 mmHg on *days 7* and *14* of ANG II infusion, respectively, in the high-dose ANG II (1,000 ng·kg^{-1}·min^{-1})-infused mice. Thus, in this study, the low dose of ANG II (200 ng·kg^{-1}·min^{-1}) corresponds to a subpressor dose, and the high dose of ANG II (1,000 ng·kg^{-1}·min^{-1}) corresponds to a pressor dose.

Suppression of ATRAP expression by ANG II in the kidney. We previously showed that ATRAP and AT1R are expressed in various mouse tissues, including the kidney, testis, and liver (42). Thus we examined whether continuous ANG II infusion would regulate ATRAP expression in a tissue-specific manner,

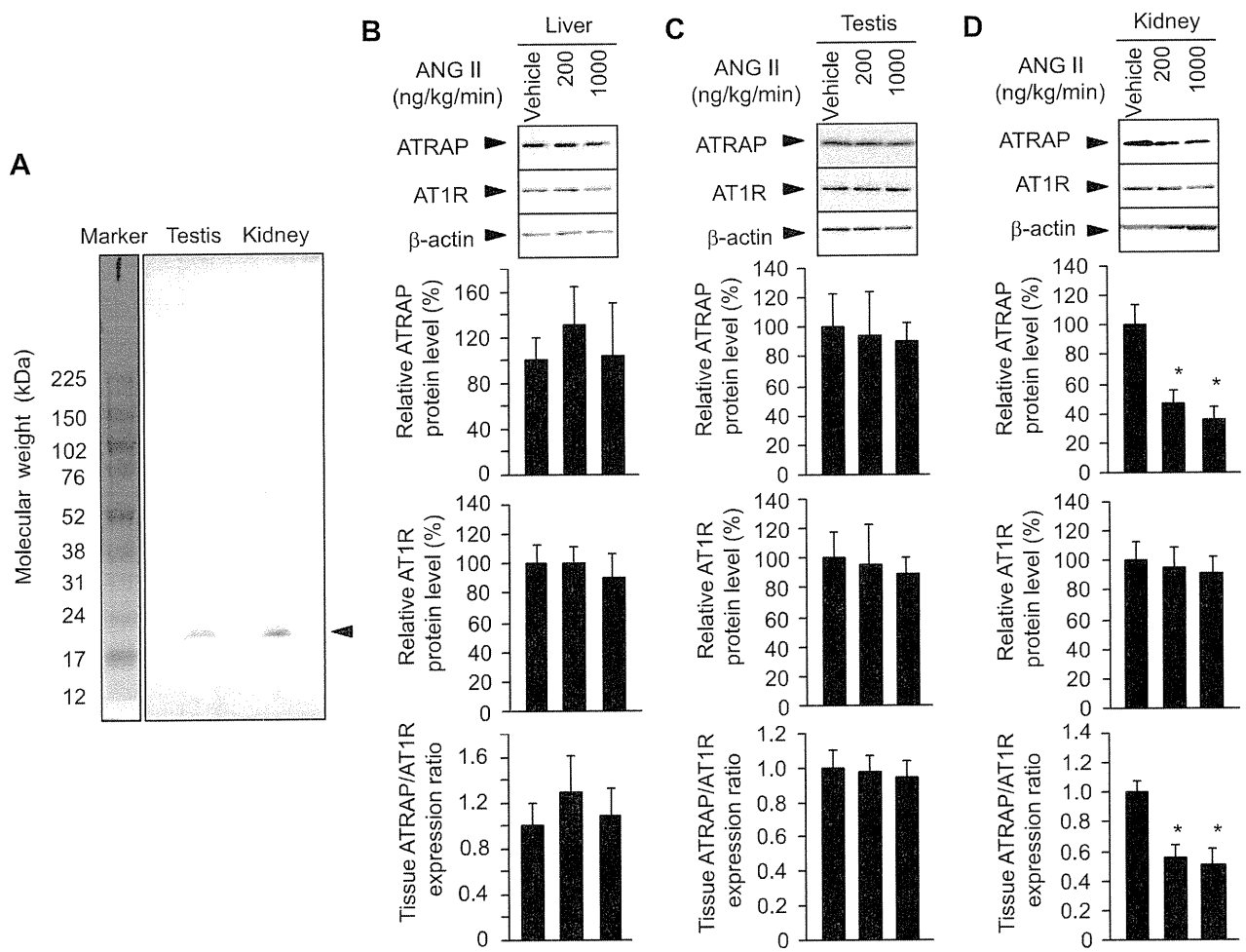

Fig. 2. Western blot showing the signal specificity of the ANG II type 1 receptor (AT1R)-associated protein (ATRAP) protein detected by the polyclonal anti-ATRAP antibody through visualization of the entire size range (*A*) and representative Western blots showing the effects of continuous ANG II infusion on the total protein expression of ATRAP and AT1R in the tissues of mice infused with vehicle or ANG II (200 or 1,000 ng·kg^{-1}·min^{-1}) for 14 days [liver (*B*); testis (*C*); kidney (*D*)]. Measurement of the ATRAP-to-AT1R ratio was performed as described in METHODS. The values were calculated relative to those obtained with extracts from mice infused with vehicle and are expressed as means ± SE ($n = 6$/group). *$P < 0.05$ vs. vehicle.

using Western blot analysis with an ATRAP-specific antibody (40, 42). Since the antibody developed against ATRAP is relatively new (42), we initially examined the signal specificity through visualization of the entire size range on Western blot analysis. Western blot analysis of tissue extracts from the testis and kidney of adult male C57BL/6 mice revealed that the polyclonal antibody for mouse ATRAP recognized a prominent band of 18 kDa, which was consistent with the predicted molecular mass of mouse ATRAP (= 18 kDa) (Fig. 2*A*).

Subsequently, we examined whether ANG II stimulation affected the expression of total ATRAP and AT1R expression using whole tissue extracts. The results of Western blot analysis showed that the hepatic and testicular protein levels of both ATRAP and AT1R were similar in the vehicle- and ANG II-infused mice, resulting in no apparent change in the relative expression ratio of ATRAP to AT1R in the liver and testis (Fig. 2, *B* and *C*). On the other hand, with respect to the renal expression of ATRAP and AT1R, although the total AT1R protein levels did not exhibit any evident change in either the vehicle-infused or ANG II-infused mice, the ATRAP protein levels at the subpressor and pressor dose in the ANG II-infused mice were significantly lower than in vehicle-infused mice after 14 days of treatment (Fig. 2*D*). As a result, the relative expression ratio of ATRAP to AT1R in the kidney was significantly suppressed at the subpressor and pressor dose in the ANG II-infused mice compared with the vehicle-infused mice (Fig. 2*D*; tissue ATRAP/AT1R expression ratio, $P < 0.05$, subpressor or pressor dose of ANG II-infused mice vs. vehicle-infused mice).

Effects of ANG II on mRNA expression of ATRAP, angiotensinogen, NADPH oxidase 4, and α-subunit of the epithelial sodium channel. We next examined the pathophysiological consequence of the observed ANG II-induced decreases in renal ATRAP expression by analyzing the mRNA expression of angiotensinogen, NADPH oxidase 4 (Nox4), and the α-subunit of the epithelial sodium channel (α-ENaC) in the kidney of the vehicle- and ANG II-infused mice. For this experiment, we also employed a higher dose of ANG II (2,500 ng·kg^{-1}·min^{-1}) for 2 wk of treatment. Systolic blood pressure was progressively elevated to 132 ± 5 and 157 ± 6 mmHg on *days 7* and *14* of ANG II infusion, respectively, from 107 ± 5 mmHg at baseline, in the higher dose ANG II (2,500 ng·kg^{-1}·min^{-1})-infused mice.

The results of real-time quantitative RT-PCR analysis showed that ANG II infusion (200, 1,000, or 2,500 ng·kg^{-1}·min^{-1}) for 14 days led to similarly significant decreases in the renal expression of the ATRAP mRNA compared with vehicle infusion (Fig. 3*A*). With respect to the renal pathological effects of ANG II stimulation, there were significant elevations of renal angiotensinogen and α-ENaC mRNA expression by ANG II infusion (2,500 ng·kg^{-1}·min^{-1}), while the renal Nox4 mRNA expression was not affected (Fig. 3, *B–D*).

Suppression of ATRAP immunostaining by ANG II in outer medulla of the kidney. We also examined the effect of ANG II infusion on the intrarenal distribution and expression levels of ATRAP by immunohistochemical analysis. The ATRAP immunohistochemical signal was detected throughout the kidney. A relatively high level of ATRAP immunoreactivity was observed in the outer medulla, and moderate ATRAP immunostaining was also observed in the renal cortex and inner medulla in vehicle-infused mice after 14 days of treatment (Fig. 4). However, there was a significant decrease in ATRAP immunoreactivity in the outer medulla of the kidney in ANG II-infused mice. This suppression of ATRAP expression was likely to be region specific in the outer medulla, since no apparent suppression of ATRAP expression was observed in the inner medulla or cortex (Fig. 4). ANG II infusion did not affect the intrarenal distribution or the relative levels of AT1R immunoreactivity (Fig. 5).

The semiquantitative evaluation with immunohistochemical analysis revealed a region-specific reduction of ATRAP immunostaining in the outer medulla with both the subpressor (200 ng·kg^{-1}·min^{-1}) and pressor (1,000 ng·kg^{-1}·min^{-1})

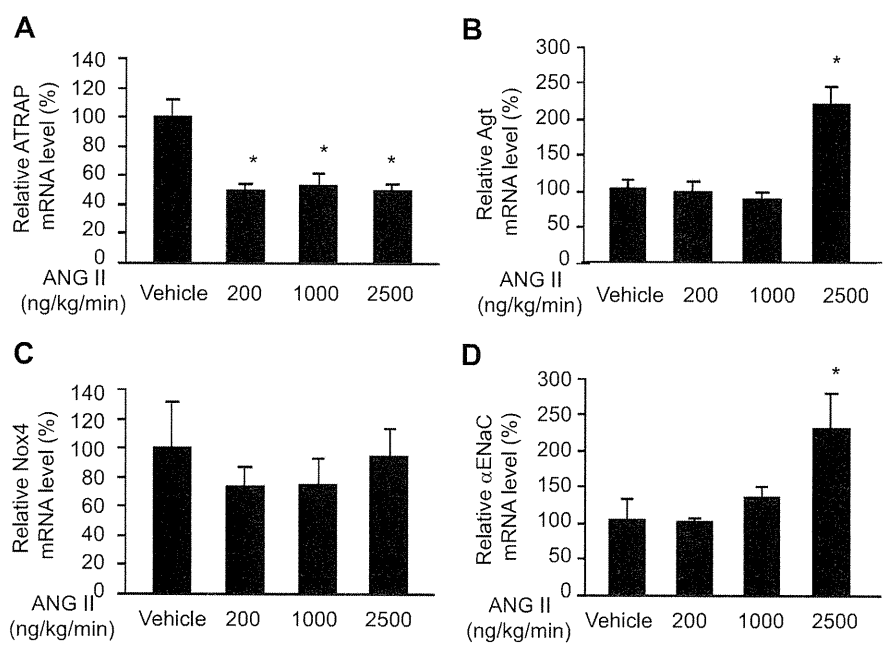

Fig. 3. Effects of continuous ANG II infusion on ATRAP (*A*), angiotensinogen (Agt; *B*), NADPH oxidase 4 (NOX4; *C*), and the α-subunit of the epithelial sodium channel (α-ENaC; *D*) mRNA expression in the mouse kidney. Real-time quantitative RT-PCR analysis shows the relative ATRAP, Agt, NOX4, and α-ENaC mRNA levels in the kidney of mice infused with vehicle or ANG II (200, 1,000, or 2,500 ng·kg^{-1}·min^{-1}) for 14 days. The values were calculated relative to those obtained with extracts from mice infused with vehicle and are expressed as means ± SE (n = 6/group). *$P < 0.05$ vs. vehicle.

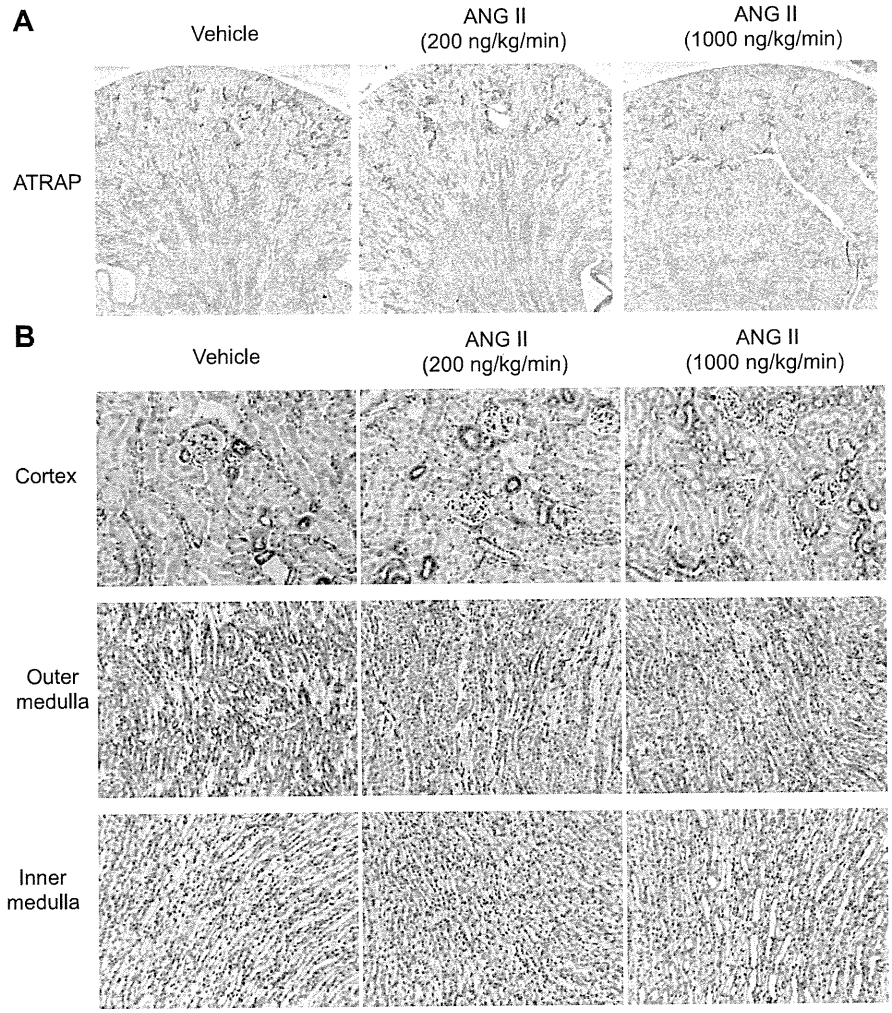

Fig. 4. Representative kidney sections showing the expression of total ATRAP protein in the kidney of mice infused with vehicle or ANG II (200 or 1,000 ng·kg^{-1}·min^{-1}) for 14 days (*A*). Positive areas for ATRAP are evident as the brown dots in the sections. Higher magnification of the kidney sections show effects of continuous ANG II infusion on the immunohistochemical localization of ATRAP expression in the renal cortex, outer medulla, and inner medulla in mice treated with vehicle or ANG II (*B*). Original magnification: ×20 (*A*); ×200 (*B*).

dose in the ANG II-infused mice, without any significant change in the pattern of intrarenal distribution or levels of AT1R immunostaining (Fig. 6). Furthermore, the results of Western blot analysis using tissue extracts from the respective kidney regions confirmed the region-specific decrease in ATRAP protein expression in the outer medulla by chronic ANG II infusion (Fig. 7).

Effects of AT1R-specific blocker olmesartan on ANG II-mediated suppression of ATRAP expression in the kidney. We further examined whether the AT1R was responsible for the ANG II infusion-mediated intrarenal suppression of ATRAP expression using the AT1R-specific blocker olmesartan. Olmesartan treatment did not affect the BW gain in mice infused with the subpressor dose (200 ng·kg^{-1}·min^{-1}, % BW increase, 20.7 ± 1.7%, n = 8), but restored normal BW gain in the mice infused with the pressor dose (1,000 ng·kg^{-1}·min^{-1}) of ANG II (% BW increase, 18.1 ± 1.6%, n = 8, $P < 0.05$, ANG II 1,000 ng·kg^{-1}·min^{-1}+olmesartan vs. ANG II 1,000 ng·kg^{-1}·min^{-1}). Olmesartan treatment also inhibited the development of hypertension in the mice treated with the pressor dose (1,000 ng·kg^{-1}·min^{-1}) of ANG II (systolic blood pressure 104 ± 6 mmHg, n = 6, $P < 0.05$, ANG II 1,000 ng·kg^{-1}·min^{-1}+olmesartan vs. ANG II 1,000 ng·kg^{-1}·min^{-1}), while olmesartan did not affect systolic blood pressure in the mice infused with the subpressor dose (200 ng·kg^{-1}·min^{-1}, 101 ± 7 mmHg, n = 6). Furthermore, olmesartan treatment completely prevented the suppressive effects of either the presser or subpressor dose of ANG II on ATRAP protein expression in the kidney (Fig. 8). No significant changes were observed in AT1R protein expression in the kidney by olmesartan treatment.

Lack of any decrease in plasma membrane AT1R expression in the kidney by chronic ANG II infusion. The results in Fig. 2 show that ANG II stimulation led to a decrease in the levels of total ATRAP protein expression in the kidney, but not other tissues, including the testis. On the other hand, the total AT1R protein expression in all of the tissues examined was unchanged by ANG II treatment (Fig. 2). Thus, to examine whether ANG II-mediated suppression of intrarenal ATRAP expression affects cell surface AT1R expression in the kidney in response to ANG II stimulation, the plasma membrane fraction was specifically extracted from the kidney and testis, and the plasma membrane AT1R protein expression was analyzed.

In the testis, the ANG II infusion at the subpressor dose (200 ng·kg^{-1}·min^{-1}) tended to decrease the expression of the plasma membrane AT1R protein, and the pressor dose (1,000

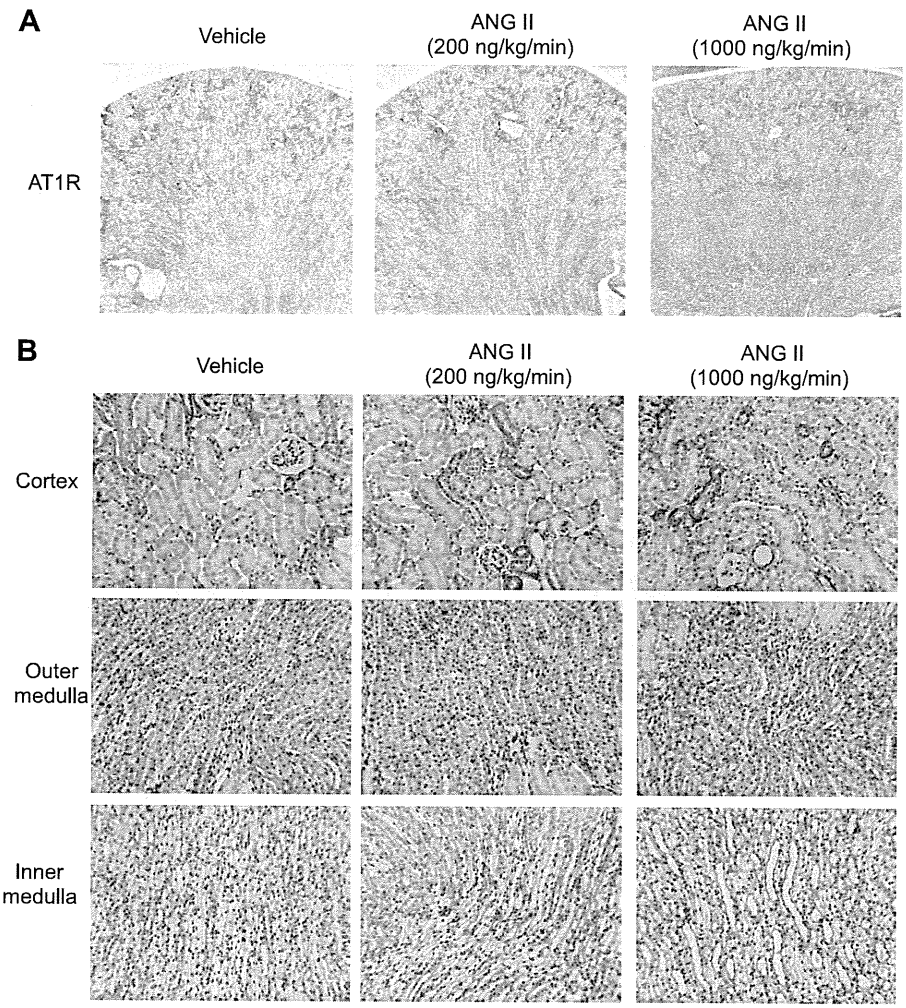

Fig. 5. Representative kidney sections showing the expression of the total AT1R protein in the kidney of mice infused with vehicle or ANG II (200 or 1,000 ng·kg^{-1}·min^{-1}) for 14 days (*A*). Positive areas for the AT1R appear as the brown dots in the sections. Higher magnification of kidney sections showing the effects of continuous ANG II infusion on immunohistochemical localization of AT1R expression in the renal cortex, outer medulla, and inner medulla in mice treated with vehicle or ANG II (*B*). Original magnification: ×20 (*A*); ×200 (*B*).

ng·kg^{-1}·min^{-1}) significantly reduced the plasma membrane AT1R protein levels (Fig. 9*A*). Since olmesartan treatment completely prevented the ANG II-induced suppressive effects on the plasma membrane AT1R protein levels in the testis (Fig. 9*A*), these results indicated that ANG II stimulation promoted AT1R internalization. In the kidney, the plasma membrane AT1R protein levels for the subpressor and pressor doses in the ANG II-infused mice were comparable to those in the vehicle-infused mice and were not affected by olmesartan treatment (Fig. 9*B*).

Decrease in plasma membrane AT1R expression in the kidney of ATRAP transgenic mice. In terms of AT1R internalization in the kidney, although ANG II stimulation decreased the ATRAP protein level and olmesartan treatment recovered it to the baseline value (Fig. 8), the plasma membrane AT1R protein level was still unaltered (Fig. 9). We hypothesized that olmesartan-mediated recovery of the downregulated ATRAP expression back to the baseline level would be insufficient to promote AT1R internalization in the kidney and that an increased expression of renal ATRAP beyond the baseline level would promote AT1R internalization and decrease plasma membrane AT1R expression. Thus, to upregulate renal ATRAP expression, we newly generated ATRAP transgenic mice using HA-tagged mouse ATRAP cDNA subcloned into the pCAGGS expression vector to test these hypotheses (Fig. 10*A*) (28).

We used these ATRAP transgenic mice for the first time to analyze a putative function of ATRAP in vivo. Western blot analysis of ATRAP expression at the protein level revealed the highest renal expression level (= 3-fold) of ATRAP (HA-ATRAP) in line 19 (Tg19), among the three lines of ATRAP transgene positive (+) mice (Fig. 10*B*), and Tg19 was therefore used for further analysis. The results of real-time quantitative RT-PCR analysis also showed a 3.7-fold increase in the baseline renal ATRAP mRNA expression over littermate control mice (Wt) in the Tg19 mice (Fig. 10*C*). While the ATRAP (HA-ATRAP) protein expression in the kidney of Tg19 mice increased compared with Wt, the total kidney AT1R protein expression in Tg19 did not differ from that in Wt (Fig. 10*D*). On the other hand, the plasma membrane AT1R protein expression in the kidney of Tg19 was significantly decreased compared with Wt at baseline (Fig. 10*E*).

Promotion of AT1R internalization and inhibition of induced expression of angiotensinogen gene in response to ANG II in the kidney of ATRAP transgenic mice. With respect to the inhibitory effect of ANG II treatment on the renal ATRAP-to-

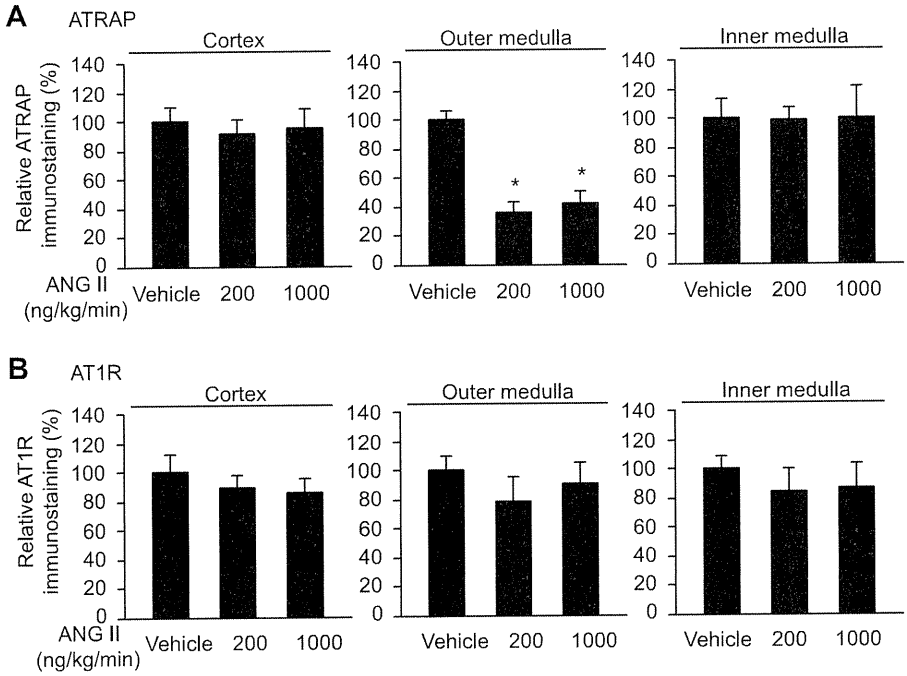

Fig. 6. Semiquantitative evaluation of the immunohistochemical analysis of ANG II-mediated effects on total ATRAP (*A*) and AT1R (*B*) protein expression in the renal cortex, outer medulla, and inner medulla in mice treated with vehicle or ANG II. The values were calculated relative to those obtained with extracts from mice infused with vehicle and are expressed as means ± SE. $*P < 0.05$ vs. vehicle.

AT1R ratio, while chronic ANG II infusion significantly decreased the ratio through a suppression of renal ATRAP expression in C57BL/6 wild-type mice (Fig. 2), ANG II treatment did not affect the ratio at all in Tg19 mice (Fig. 11*A*). Regarding AT1R internalization in the kidney, while the plasma membrane AT1R protein level was not affected by either chronic ANG II stimulation or olmesartan treatment in C57BL/6 wild-type mice (Figs. 8 and 9), it was significantly decreased by ANG II infusion in Tg19 (Fig. 11*B*), thereby indicating that enhancement of renal ATRAP expression beyond baseline promotes AT1R internalization.

Since the body size and BW of Tg19 mice were not different from the Wt at baseline (data not shown), we finally examined the physiological effects of overexpression of ATRAP in Tg19 with respect to blood pressure, response to ANG II, and target organ effects. The systolic blood pressure of Tg19 mice was comparable with that of Wt at baseline, and chronic ANG II infusion significantly and similarly increased systolic blood pressure in Tg19 and Wt (Fig. 11*C*). However, while ANG II infusion in Wt increased the angiotensinogen mRNA expression level in the kidney by 2.25-fold, the mRNA upregulation in response to ANG II infusion was significantly inhibited in Tg19 (Fig. 11*D*). These results indicate that the renal enhancement of ATRAP expression inhibits the ANG II-mediated activation of renal angiotensinogen gene expression, most likely through a promotion of AT1R internalization in response to ANG II.

DISCUSSION

The present data show that either a subpressor or pressor infusion of ANG II in mice causes a significant suppression of intrarenal ATRAP expression and that this response is dependent on the activation of AT1R. The decrease in intrarenal ATRAP expression during continuous ANG II infusion was demonstrated at the mRNA level by quantitative real-time RT-PCR, and at the protein level by Western blotting, and was supported by immunohistochemistry. In addition, the ANG II-mediated decrease in renal ATRAP expression through AT1R signaling occurred concomitantly with the lack of ANG II-induced decrease in plasma membrane AT1R expression in the kidney. Furthermore, a transgenic model increase in renal ATRAP expression beyond baseline expression was accompanied by a reduction in plasma membrane AT1R expression in the kidney, and by the promotion of renal AT1R internalization and the inhibition of an increase in renal angiotensinogen gene expression in response to ANG II.

Several previous studies have reported that activation of the intrarenal renin-angiotensin system and the AT1R pathway plays an important role in the pathogenesis of hypertension and renal injury (19, 25, 33). With respect to the mechanisms involved in ANG II-induced hypertension, the AT1R-mediated enhancement of renal angiotensinogen, collecting duct renin, intrarenal ANG II levels, medullary oxidative stress, and the failure to downregulate renal AT1R expression levels are all reported to be involved in the sustained effects of continuous ANG II elevation on eliciting hypertension (12, 13, 20, 23, 31, 50). Because the biological actions of ANG II are influenced by the AT1R expression levels, and ANG II infusion in mice specifically lacking AT1R in the kidney failed to develop hypertension (6), investigation of the renal activity of AT1R signaling in ANG II-induced hypertension is important to elucidate the mechanisms responsible for the cardiovascular and renal functional changes observed in this hypertension model.

We previously cloned ATRAP as a novel molecule which interacts with AT1R and showed that ATRAP suppressed ANG II-induced hypertrophic and proliferative responses of cardiovascular cells by inducing a constitutive internalization

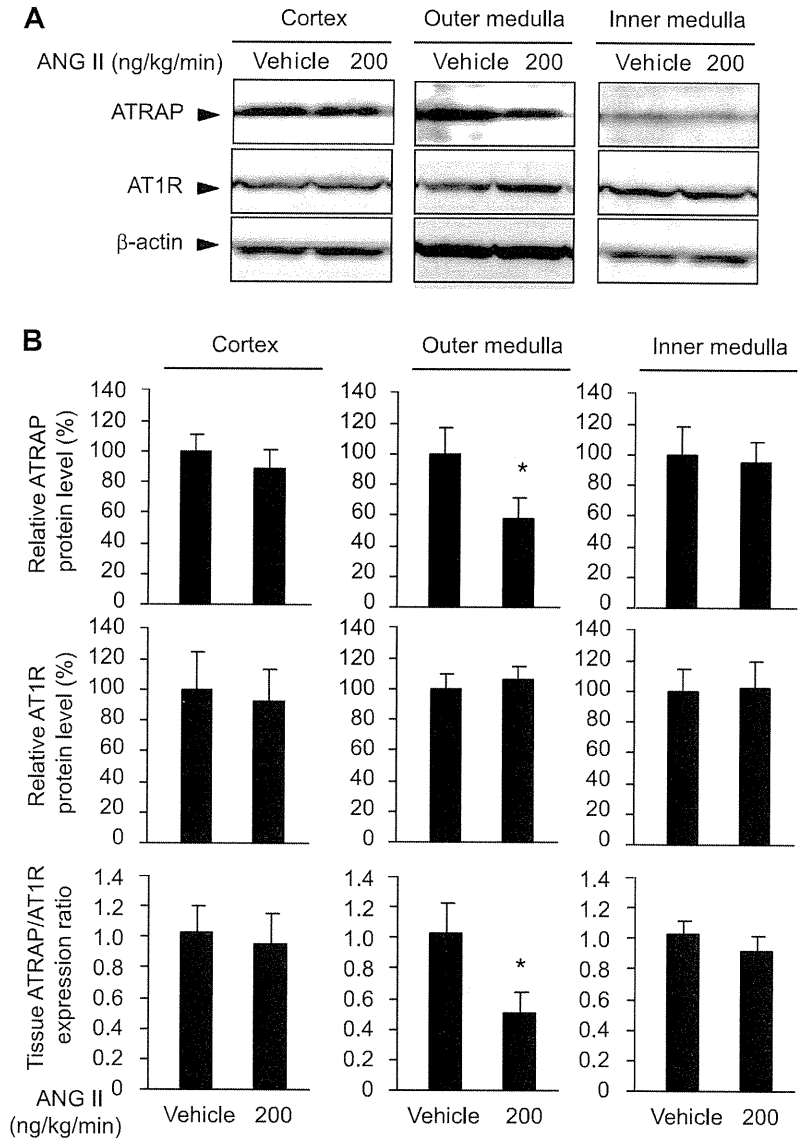

Fig. 7. Representative Western blots showing the effects of continuous ANG II infusion on the total protein expression of ATRAP and AT1R in the renal cortex, outer medulla, and inner medulla in mice infused with vehicle or ANG II (200 ng·kg^{-1}·min^{-1}) for 14 days (*A*). Measurement of the ATRAP-to-AT1R ratio was performed as described in METHODS (*B*). The values were calculated relative to those obtained with extracts from mice infused with vehicle and are expressed as means ± SE (n = 6/group). *P < 0.05 vs. vehicle.

of AT1R (22, 37). Thus a tissue-specific regulatory balancing of ATRAP and AT1R expression may be involved in the modulation of AT1R signaling in each tissue. We previously showed that ATRAP is expressed in a variety of mouse tissues, as is the AT1R, and that dietary salt intake modulates renal ATRAP expression (42). In this study, the expression of the hepatic and testicular ATRAP protein was not affected by continuous ANG II infusion. Although activation of the tissue renin-angiotensin system is important for the pathogenesis of hypertension and is associated with organ injury, the liver and testis are not target organs of hypertensive tissue injury. Our previous studies showed that the progression of hypertension did not affect hepatic angiotensinogen gene expression in genetically hypertensive rats, which is consistent with the results in the present study (38, 39).

In terms of the regulation of the intrarenal renin-angiotensin system by ANG II stimulation, previous studies by Navar and others (9, 20, 25, 27) established that ANG II is accumulated in the kidney of rats upon infusion, a response that is prevented by AT1R-specific blockers. Further evidence from experiments using rats suggests that AT1R-specific blockers decrease intrarenal ANG II levels by preventing AT1R-mediated uptake, as well as AT1R-mediated induction of intrarenal angiotensinogen, which is a substrate of ANG II (26). We previously showed that ATRAP is abundantly expressed and widely distributed along the renal tubules from Bowman's capsule to the inner medullary collecting ducts in mice (42). In this study, while continuous ANG II infusion did not have any apparent effects on renal total AT1R protein expression in C57BL/6 wild-type mice, which is consistent with previous reports using rats (12, 13), there was a significant decrease in renal ATRAP expression in ANG II-infused mice, and thereby a marked suppression of the renal expression ratio of ATRAP to AT1R at a subpressor dose of ANG II, even without an increase in blood pressure. This suppression of the renal ATRAP expression by ANG II is AT1R dependent, as it is prevented by treatment with olmesartan.

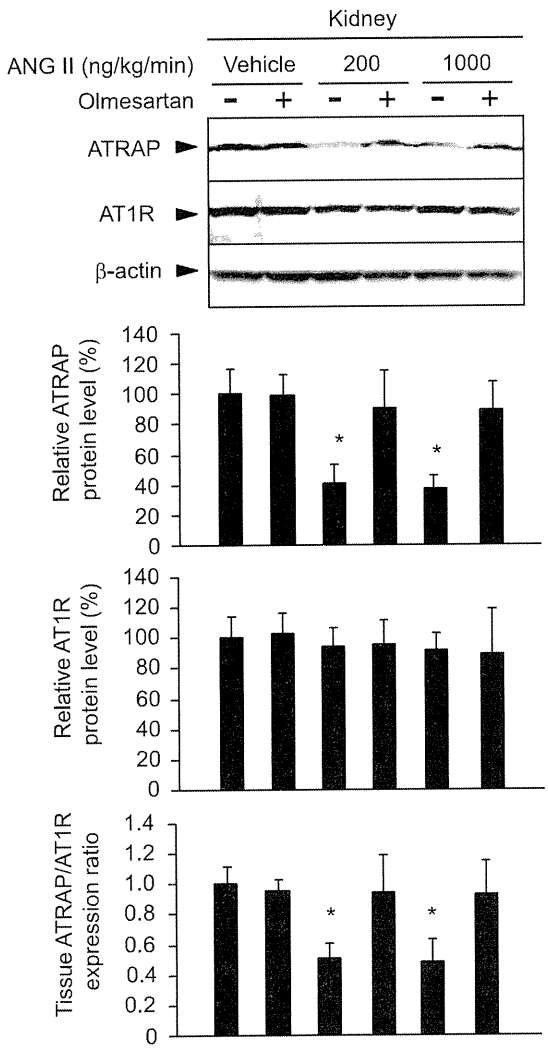

Fig. 8. Representative Western blots showing the effects of continuous ANG II infusion on the total protein expression of ATRAP and AT1R in the kidney of mice infused with vehicle or ANG II (200 or 1,000 ng·kg^{-1}·min^{-1}) with or without olmesartan treatment (10 mg·kg^{-1}·day^{-1} in the drinking water) for 14 days. Measurement of the ATRAP-to-AT1R ratio was performed as described in METHODS. The values were calculated relative to those obtained with extracts from mice infused with vehicle without olmesartan and are expressed as means ± SE (n = 6/group). *P < 0.05 vs. vehicle without olmesartan.

Previous studies also showed that chronic ANG II stimulation in rats leads to the activation of the intrarenal renin-angiotensin system, with an augmentation of renal angiotensinogen expression (20), enhancement of oxidative stress through increases in NADPH oxidase activity (3, 4), and increases in sodium retention through an upregulation of α-ENaC expression (2). On the other hand, a previous study reported that the mouse kidney is relatively resistant to ANG II, including oxidative stress, compared with the rat kidney (45). In the present study, intrarenal angiotensinogen, NADPH oxidase, and α-ENaC mRNA expression was not significantly affected by ANG II infusion of either the subpressor (200 ng·kg^{-1}·min^{-1}) or pressor dose (1,000 ng·kg^{-1}·min^{-1}) for 2 wk, despite a decrease in renal ATRAP expression.

Thus we next employed a higher dose of ANG II (2,500 ng·kg^{-1}·min^{-1}) for 2 wk of treatment, which was recently shown to cause hypertension and renal injury even in mice (46), and showed that it did provoke progressive blood pressure increases and pathological renal responses, including elevated expression levels of renal angiotensinogen and α-ENaC genes, along with a concomitant decrease in renal ATRAP expression (Fig. 3). These observations suggest that a decrease in renal ATRAP expression might be a preceding renal marker of pathological responses to ANG II stimulation in vivo. Nevertheless, because ANG II infusion of the subpressor dose already exerted a down-regulatory effect on renal ATRAP expression without increases in the renal mRNA level of angiotensinogen and α-ENaC, there was a lack of any direct relationship between ATRAP and the expression of angio-

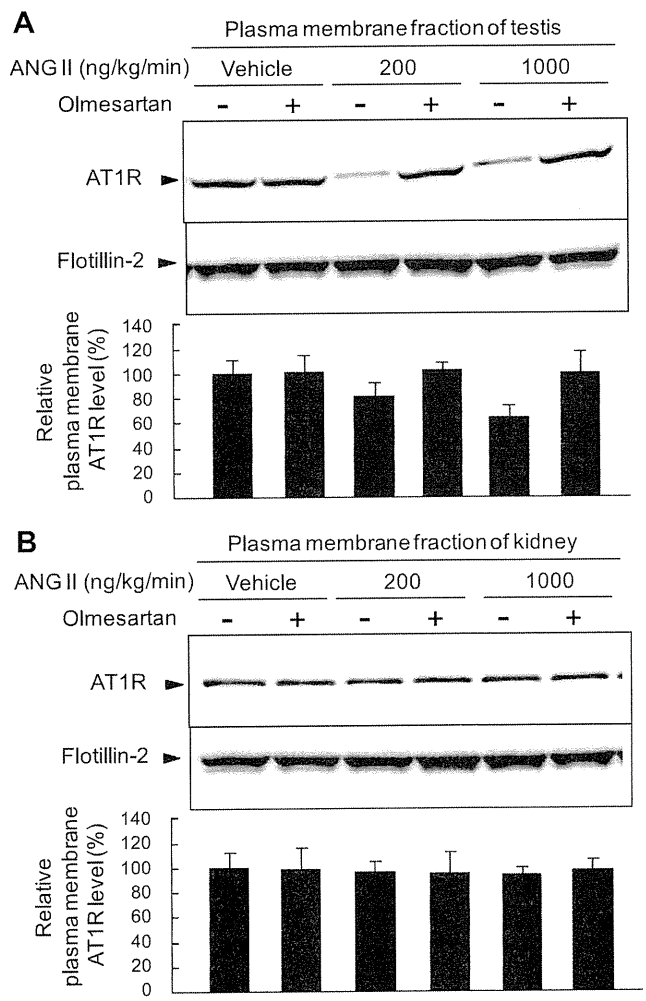

Fig. 9. Representative Western blots showing the effects of continuous ANG II infusion on the plasma membrane AT1R protein level in the tissues of mice infused with vehicle or ANG II (200 or 1,000 ng·kg^{-1}·min^{-1}) with or without olmesartan treatment (10 mg·kg^{-1}·day^{-1} in the drinking water) for 14 days [testis (*A*); kidney (*B*)]. Flotillin-2 is constitutively localized to the plasma membrane and is an internal control protein. The values were calculated relative to those using plasma membrane fractions from mice infused with vehicle without olmesartan and are expressed as means ± SE (n = 6/group). *P < 0.05 vs. vehicle without olmesartan.

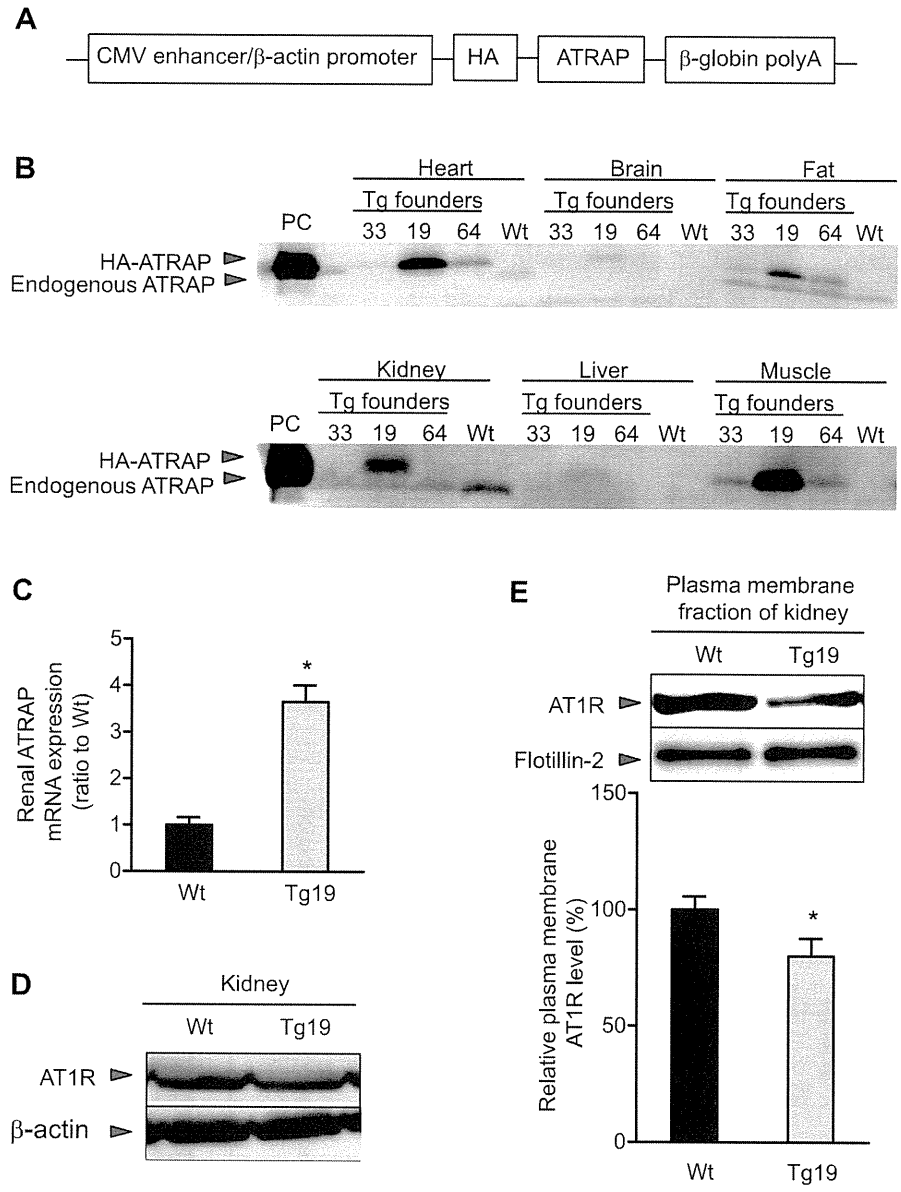

Fig. 10. Generation of ATRAP transgenic mice and decrease in the plasma membrane AT1R expression in the kidney. *A*: transgenic mice expressing ATRAP were generated on a C57BL/6J background with standard techniques. Briefly, the hemagglutinin (HA)-tagged mouse ATRAP cDNA was subcloned into the pCAGGS expression vector, which contained the cytomegalovirus (CMV) enhancer and chicken β-actin (CAG) promoter, and the resultant transgene construct was microinjected into the pronuclei of fertilized mouse embryos at the single-cell stage to generate transgenic mice (C57BL/6 strain). *B*: Western blot analysis of ATRAP expression at the protein level revealed the highest renal expression level (= 3-fold) of ATRAP (HA-ATRAP) in line 19 (Tg19), among the 3 lines of ATRAP transgene positive (+) mice obtained. Tg19 was used for further analysis in the present study. *C*: results of real-time quantitative RT-PCR analysis showed a 3.7-fold increase in the baseline renal ATRAP mRNA expression over littermate control mice (Wt) in ATRAP transgenic mice (Tg19). The values were calculated relative to those in kidneys from Wt and are expressed as means ± SE (n = 7/group). *$P < 0.05$ vs. Wt. *D*: results of Western blot analysis showed that the total kidney AT1R protein expression of Tg19 did not differ from that in Wt. *E*: results of Western blot analysis showed that the plasma membrane AT1R protein expression in the kidney of Tg19 was significantly decreased compared with Wt at baseline. The values were calculated relative to those from the plasma membrane fractions of Wt and are expressed as means ± SE (n = 9/group). *$P < 0.05$ vs. Wt.

tensinogen and α-ENaC genes in the kidney. Thus the results did not establish any causality or effect with respect to changes in renal ATRAP at this stage. Therefore, further investigation is needed to elucidate the exact molecular causal relationship between them.

The results of immunohistochemistry, including semiquantitative evaluation and Western blot analysis using the respective kidney regions, revealed a reduction of ATRAP expression in the outer medulla resulting from ANG II stimulation. Since previous studies showed that the outer medulla plays an important role in ANG II-mediated renal injury (23, 24), the suppression of renal ATRAP, particularly in the outer medullary region, may play a role in the renal pathological responses elicited by ANG II stimulation. While the intrarenal colocalization of ATRAP with AT1R suggests a functional role for ATRAP, it does not necessarily implicate ATRAP in electrolyte transport, renal injury, or hypertension, and the precise tubular function of ATRAP remains to be determined. The detailed molecular mechanism responsible for the tissue-specific AT1R-mediated suppression of ATRAP expression is still unclear. Further studies are necessary to determine the regulatory machinery of ATRAP gene transcription, including the transcription factors interacting with the promoter region of ATRAP gene and the functional effects of ATRAP on ANG II-mediated pathological responses using cultured renal tubular cells, and such studies are now underway.

Previous in vitro results suggested that ATRAP promotes AT1R internalization so as to inhibit AT1R signaling (37). In the present study, chronic ANG II infusion with either the a low or high dose caused significant suppression of endogenous ATRAP expression in the kidney, but not in the testis (Fig. 2).

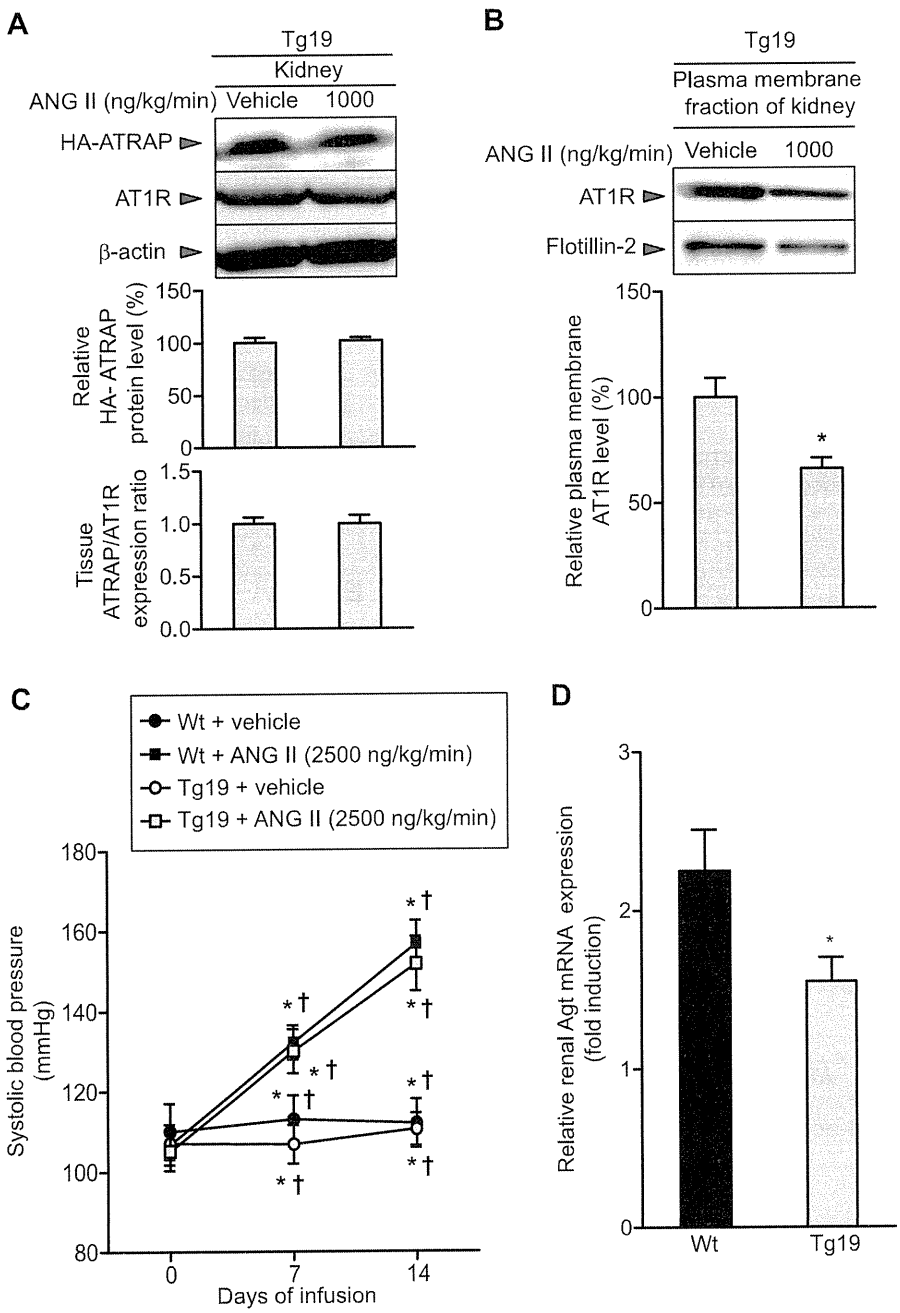

Fig. 11. Promotion of AT1R internalization and inhibition of induced expression of angiotensinogen gene in response to ANG II in the kidney of ATRAP transgenic mice. *A*: representative Western blots showing the effects of continuous ANG II infusion on the total protein expression of HA-ATRAP and AT1R in the kidney of ATRAP transgenic mice (Tg19) infused with vehicle or ANG II (1,000 $ng \cdot kg^{-1} \cdot min^{-1}$) for 14 days. Measurement of the ATRAP-to-AT1R ratio was performed as described in METHODS, and the values were calculated relative to those in extracts from Tg19 infused with vehicle and are expressed as means ± SE (n = 6/group). *B*: representative Western blots showing the effects of ANG II infusion on the plasma membrane AT1R protein level in the kidney of Tg19 infused with vehicle or ANG II (1,000 $ng \cdot kg^{-1} \cdot min^{-1}$) for 14 days. The values were calculated relative to those obtained with extracts from Tg19 infused with vehicle and are expressed as means ± SE (n = 6/group). *C*: effects of ANG II infusion on systolic blood pressure during the treatment period. Tg19 and littermate control mice (Wt) were infused with either vehicle or ANG II (2,500 $ng \cdot kg^{-1} \cdot min^{-1}$) for 14 days. The values of systolic blood pressure are expressed as means ± SE (n = 6/group). *$P < 0.05$ vs. vehicle. †$P < 0.05$ vs. *day 0*. *D*: effects of ANG II infusion on renal Agt mRNA expression in Wt and Tg19. Values are calculated as the fold-induction of those from extracts in the vehicle-infused mice and are expressed as means ± SE (n = 6/group). *$P < 0.05$ vs. Wt.

On the other hand, ANG II infusion did not alter plasma membrane AT1R expression in the kidney but significantly decreased it in the testis (Fig. 8), while total AT1R expression was not altered by ANG II in either of these tissues (Fig. 2). As a result, it is probable that testicular ATRAP promoted substantial ANG II-induced AT1R internalization, which was estimated by comparing the plasma membrane AT1R level with the total AT1R level.

In terms of AT1R internalization in the kidney, although ANG II downregulated ATRAP expression and olmesartan treatment recovered it to the baseline level (Fig. 8), the plasma membrane AT1R expression itself was not affected at all (Fig. 9), thereby still indicating the possibility that renal ATRAP exerts no effect on AT1R internalization in the kidney. We hypothesized that upregulation of renal ATRAP expression beyond baseline promotes AT1R internalization such that it is detected as a decrease in plasma membrane AT1R expression in the kidney without a change in the total AT1R protein level.

Thus, to examine the ATRAP-mediated effect on renal AT1R internalization by a different strategy in vivo, we produced ATRAP transgenic mice. The results demonstrated that enhancement of renal ATRAP expression in transgenic mice caused a decrease in the plasma membrane AT1R level, even at baseline without ANG II stimulation, irrespective of there

being no change in the total AT1R level in the kidney (Fig. 10). Furthermore, the results of ANG II infusion experiments showed that the plasma membrane AT1R level was further decreased by ANG II stimulation in the kidney of ATRAP transgenic mice (Fig. 11), which was accompanied by a decreased response of renal angiotensinogen mRNA expression to ANG II. This is in contrast to there being no change in the plasma membrane AT1R level by ANG II in the kidney of wild-type mice (Fig. 9). These results collectively suggest that enhancement of renal ATRAP expression beyond baseline promotes AT1R internalization in response to ANG II. A recent study by Oppermann et al. (29) also showed that a genetic deficiency of ATRAP in mice caused an enhanced surface expression of AT1R in the kidney, which is consistent with the results in this study.

The results of the present study show that continuous ANG II infusion decreased intrarenal ATRAP expression through ANG II-mediated AT1R signaling, particularly in the outer medulla, with the lack of any decrease in plasma membrane AT1R expression in the kidney in C57BL/6 wild-type mice. On the other hand, transgenic overexpression of ATRAP reduced the plasma membrane AT1R level in the kidney at baseline and further decreased the plasma membrane AT1R expression in response to ANG II stimulation, concomitant with the decreased ANG II-induced response of the angiotensinogen gene, despite there being no change in the total AT1R level.

Nevertheless, a limitation of the present study is that our findings strongly suggest that ATRAP at supraphysiological levels can alter the plasma membrane levels of AT1R at baseline and in response to ANG II stimulation, but with no detectable physiological effect on blood pressure. Target organ effects such as proteinuria and degree of renal damage by histological examination were not analyzed in this study. The only detectable consequence was a difference in angiotensinogen mRNA expression in response to ANG II stimulation, but it remains unclear whether this would translate to a difference in angiotensinogen protein levels.

In conclusion, these results suggest that AT1R and ATRAP modulate each other, at least in the kidney, and that activation of AT1R signaling has a dominant effect over endogenous renal ATRAP under chronic ANG II infusion, but that renal ATRAP activation by a transgenic model that increases ATRAP expression beyond baseline may cause a constitutive reduction of plasma membrane AT1R expression and a promotion of AT1R internalization in response to ANG II. Further studies to analyze downstream signaling events mediated by activation of AT1R under the condition of ATRAP overexpression are warranted to elucidate the detailed molecular mechanisms and pathophysiological significance of ATRAP-mediated inhibition of AT1R signaling in vivo.

ACKNOWLEDGMENTS

The authors thank Emi Maeda and Hiroko Morinaga for technical assistance and helpful discussion. The authors also thank Dr. Kevin Boru for English editing of this manuscript.

GRANTS

This work was supported in part by grants from the Japanese Ministry of Education, Science, Sports, and Culture, by a Health and Labor Sciences Research grant, and by grants from the Salt Science Research Foundation (1033), the Mitsubishi Pharma Research Foundation, and the Strategic Research Project of Yokohama City University.

DISCLOSURES

No conflicts of interest, financial or otherwise, are declared by the authors.

REFERENCES

1. **Azuma K, Tamura K, Shigenaga A, Wakui H, Masuda S, Tsurumi-Ikeya Y, Tanaka Y, Sakai M, Matsuda M, Hashimoto T, Ishigami T, Lopez-Ilasaca M, Umemura S.** Novel regulatory effect of angiotensin II type 1 receptor-interacting molecule on vascular smooth muscle cells. *Hypertension* 50: 926–932, 2007.
2. **Beutler KT, Masilamani S, Turban S, Nielsen J, Brooks HL, Ageloff S, Fenton RA, Packer RK, Knepper MA.** Long-term regulation of ENaC expression in kidney by angiotensin II. *Hypertension* 41: 1143–1150, 2003.
3. **Block K, Eid A, Griendling KK, Lee DY, Wittrant Y, Gorin Y.** Nox4 NAD(P)H oxidase mediates Src-dependent tyrosine phosphorylation of PDK-1 in response to angiotensin II: role in mesangial cell hypertrophy and fibronectin expression. *J Biol Chem* 283: 24061–24076, 2008.
4. **Chabrashvili T, Kitiyakara C, Blau J, Karber A, Aslam S, Welch WJ, Wilcox CS.** Effects of ANG II type 1 and 2 receptors on oxidative stress, renal NADPH oxidase, and SOD expression. *Am J Physiol Regul Integr Comp Physiol* 285: R117–R124, 2003.
5. **Coffman TM, Crowley SD.** Kidney in hypertension: guyton redux. *Hypertension* 51: 811–816, 2008.
6. **Crowley SD, Gurley SB, Herrera MJ, Ruiz P, Griffiths R, Kumar AP, Kim HS, Smithies O, Le TH, Coffman TM.** Angiotensin II causes hypertension and cardiac hypertrophy through its receptors in the kidney. *Proc Natl Acad Sci USA* 103: 17985–17990, 2006.
7. **Cui T, Nakagami H, Iwai M, Takeda Y, Shiuchi T, Tamura K, Daviet L, Horiuchi M.** ATRAP, novel AT1 receptor associated protein, enhances internalization of AT1 receptor and inhibits vascular smooth muscle cell growth. *Biochem Biophys Res Commun* 279: 938–941, 2000.
8. **Daviet L, Lehtonen JY, Tamura K, Griese DP, Horiuchi M, Dzau VJ.** Cloning and characterization of ATRAP, a novel protein that interacts with the angiotensin II type 1 receptor. *J Biol Chem* 274: 17058–17062, 1999.
9. **Gonzalez-Villalobos RA, Satou R, Seth DM, Semprun-Prieto LC, Katsurada A, Kobori H, Navar LG.** Angiotensin-converting enzyme-derived angiotensin II formation during angiotensin II-induced hypertension. *Hypertension* 53: 351–355, 2009.
10. **Gonzalez-Villalobos RA, Seth DM, Satou R, Horton H, Ohashi N, Miyata K, Katsurada A, Tran DV, Kobori H, Navar LG.** Intrarenal angiotensin II and angiotensinogen augmentation in chronic angiotensin II-infused mice. *Am J Physiol Renal Physiol* 295: F772–F779, 2008.
11. **Guo S, Lopez-Ilasaca M, Dzau VJ.** Identification of calcium-modulating cyclophilin ligand (CAML) as transducer of angiotensin II-mediated nuclear factor of activated T cells (NFAT) activation. *J Biol Chem* 280: 12536–12541, 2005.
12. **Harrison-Bernard LM, El-Dahr SS, O'Leary DF, Navar LG.** Regulation of angiotensin II type 1 receptor mRNA and protein in angiotensin II-induced hypertension. *Hypertension* 33: 340–346, 1999.
13. **Harrison-Bernard LM, Zhuo J, Kobori H, Ohishi M, Navar LG.** Intrarenal AT_1 receptor and ACE binding in ANG II-induced hypertensive rats. *Am J Physiol Renal Physiol* 282: F19–F25, 2002.
14. **Hirose T, Satoh D, Kurihara H, Kusaka C, Hirose H, Akimoto K, Matsusaka T, Ichikawa I, Noda T, Ohno S.** An essential role of the universal polarity protein, aPKClambda, on the maintenance of podocyte slit diaphragms. *PLoS One* 4: e4194, 2009.
15. **Hong SW, Isono M, Chen S, Iglesias-De La Cruz MC, Han DC, Ziyadeh FN.** Increased glomerular and tubular expression of transforming growth factor-beta1, its type II receptor, and activation of the Smad signaling pathway in the db/db mouse. *Am J Pathol* 158: 1653–1663, 2001.
16. **Hunyady L, Bor M, Balla T, Catt KJ.** Identification of a cytoplasmic Ser-Thr-Leu motif that determines agonist-induced internalization of the AT1 angiotensin receptor. *J Biol Chem* 269: 31378–31382, 1994.
17. **Iwamoto T, Kita S, Zhang J, Blaustein MP, Arai Y, Yoshida S, Wakimoto K, Komuro I, Katsuragi T.** Salt-sensitive hypertension is triggered by Ca^{2+} entry via Na^+/Ca^{2+} exchanger type-1 in vascular smooth muscle. *Nat Med* 10: 1193–1199, 2004.

18. **Kagiyama S, Matsumura K, Fukuhara M, Sakagami K, Fujii K, Iida M.** Aldosterone-and-salt-induced cardiac fibrosis is independent from angiotensin II type 1a receptor signaling in mice. *Hypertens Res* 30: 979–989, 2007.
19. **Kobori H, Nangaku M, Navar LG, Nishiyama A.** The intrarenal renin-angiotensin system: from physiology to the pathobiology of hypertension and kidney disease. *Pharmacol Rev* 59: 251–287, 2007.
20. **Kobori H, Prieto-Carrasquero MC, Ozawa Y, Navar LG.** AT1 receptor mediated augmentation of intrarenal angiotensinogen in angiotensin II-dependent hypertension. *Hypertension* 43: 1126–1132, 2004.
21. **Lopez-Ilasaca M, Liu X, Tamura K, Dzau VJ.** The angiotensin II type I receptor-associated protein, ATRAP, is a transmembrane protein and a modulator of angiotensin II signaling. *Mol Biol Cell* 14: 5038–5050, 2003.
22. **Mogi M, Iwai M, Horiuchi M.** Emerging concepts of regulation of angiotensin II receptors: new players and targets for traditional receptors. *Arterioscler Thromb Vasc Biol* 27: 2532–2539, 2007.
23. **Mori T, Cowley AW Jr.** Angiotensin II-NAD(P)H oxidase-stimulated superoxide modifies tubulovascular nitric oxide cross-talk in renal outer medulla. *Hypertension* 42: 588–593, 2003.
24. **Mori T, O'Connor PM, Abe M, Cowley AW Jr.** Enhanced superoxide production in renal outer medulla of Dahl salt-sensitive rats reduces nitric oxide tubular-vascular cross-talk. *Hypertension* 49: 1336–1341, 2007.
25. **Navar LG, Harrison-Bernard LM, Nishiyama A, Kobori H.** Regulation of intrarenal angiotensin II in hypertension. *Hypertension* 39: 316–322, 2002.
26. **Nishiyama A, Nakagawa T, Kobori H, Nagai Y, Okada N, Konishi Y, Morikawa T, Okumura M, Meda I, Kiyomoto H, Hosomi N, Mori T, Ito S, Imanishi M.** Strict angiotensin blockade prevents the augmentation of intrarenal angiotensin II and podocyte abnormalities in type 2 diabetic rats with microalbuminuria. *J Hypertens* 26: 1849–1859, 2008.
27. **Nishiyama A, Seth DM, Navar LG.** Angiotensin II type 1 receptor-mediated augmentation of renal interstitial fluid angiotensin II in angiotensin II-induced hypertension. *J Hypertens* 21: 1897–1903, 2003.
28. **Niwa H, Yamamura K, Miyazaki J.** Efficient selection for high-expression transfectants with a novel eukaryotic vector. *Gene* 108: 193–199, 1991.
29. **Oppermann M, Gess B, Schweda F, Castrop H.** Atrap deficiency increases arterial blood pressure and plasma volume. *J Am Soc Nephrol* 21: 468–477, 2010.
30. **Oshita A, Iwai M, Chen R, Ide A, Okumura M, Fukunaga S, Yoshii T, Mogi M, Higaki J, Horiuchi M.** Attenuation of inflammatory vascular remodeling by angiotensin II type 1 receptor-associated protein. *Hypertension* 48: 671–676, 2006.
31. **Prieto-Carrasquero MC, Kobori H, Ozawa Y, Gutierrez A, Seth D, Navar LG.** AT_1 receptor-mediated enhancement of collecting duct renin in angiotensin II-dependent hypertensive rats. *Am J Physiol Renal Physiol* 289: F632–F637, 2005.
32. **Reich HN, Oudit GY, Penninger JM, Scholey JW, Herzenberg AM.** Decreased glomerular and tubular expression of ACE2 in patients with type 2 diabetes and kidney disease. *Kidney Int* 74: 1610–1616, 2008.
33. **Rohrwasser A, Morgan T, Dillon HF, Zhao L, Callaway CW, Hillas E, Zhang S, Cheng T, Inagami T, Ward K, Terreros DA, Lalouel JM.** Elements of a paracrine tubular renin-angiotensin system along the entire nephron. *Hypertension* 34: 1265–1274, 1999.
34. **Sakai M, Tamura K, Tsurumi Y, Tanaka Y, Koide Y, Matsuda M, Ishigami T, Yabana M, Tokita Y, Hiroi Y, Komuro I, Umemura S.** Expression of MAK-V/Hunk in renal distal tubules and its possible involvement in proliferative suppression. *Am J Physiol Renal Physiol* 292: F1526–F1536, 2007.
35. **Shigenaga A, Tamura K, Wakui H, Masuda S, Azuma K, Tsurumi-Ikeya Y, Ozawa M, Mogi M, Matsuda M, Uchino K, Kimura K, Horiuchi M, Umemura S.** Effect of olmesartan on tissue expression balance between angiotensin II receptor and its inhibitory binding molecule. *Hypertension* 52: 672–678, 2008.
36. **Solis GP, Hoegg M, Munderloh C, Schrock Y, Malaga-Trillo E, Rivera-Milla E, Stuermer CA.** Reggie/flotillin proteins are organized into stable tetramers in membrane microdomains. *Biochem J* 403: 313–322, 2007.
37. **Tamura K, Tanaka Y, Tsurumi Y, Azuma K, Shigenaga A, Wakui H, Masuda S, Matsuda M.** The role of angiotensin AT1 receptor-associated protein in renin-angiotensin system regulation and function. *Curr Hypertens Rep* 9: 121–127, 2007.
38. **Tamura K, Umemura S, Nyui N, Yamakawa T, Yamaguchi S, Ishigami T, Tanaka S, Tanimoto K, Takagi N, Sekihara H, Murakami K, Ishii M.** Tissue-specific regulation of angiotensinogen gene expression in spontaneously hypertensive rats. *Hypertension* 27: 1216–1223, 1996.
39. **Tamura K, Umemura S, Yamakawa T, Nyui N, Hibi K, Watanabe Y, Ishigami T, Yabana M, Tanaka S, Sekihara H, Murakami K, Ishii M.** Modulation of tissue angiotensinogen gene expression in genetically obese hypertensive rats. *Am J Physiol Regul Integr Comp Physiol* 272: R1704–R1711, 1997.
40. **Tanaka Y, Tamura K, Koide Y, Sakai M, Tsurumi Y, Noda Y, Umemura M, Ishigami T, Uchino K, Kimura K, Horiuchi M, Umemura S.** The novel angiotensin II type 1 receptor (AT1R)-associated protein ATRAP downregulates AT1R and ameliorates cardiomyocyte hypertrophy. *FEBS Lett* 579: 1579–1586, 2005.
41. **Tang H, Guo DF, Porter JP, Wanaka Y, Inagami T.** Role of cytoplasmic tail of the type 1A angiotensin II receptor in agonist- and phorbol ester-induced desensitization. *Circ Res* 82: 523–531, 1998.
42. **Tsurumi Y, Tamura K, Tanaka Y, Koide Y, Sakai M, Yabana M, Noda Y, Hashimoto T, Kihara M, Hirawa N, Toya Y, Kiuchi Y, Iwai M, Horiuchi M, Umemura S.** Interacting molecule of AT1 receptor, ATRAP, is colocalized with AT1 receptor in the mouse renal tubules. *Kidney Int* 69: 488–494, 2006.
43. **Vila-Carriles WH, Kovacs GG, Jovov B, Zhou ZH, Pahwa AK, Colby G, Esimai O, Gillespie GY, Mapstone TB, Markert JM, Fuller CM, Bubien JK, Benos DJ.** Surface expression of ASIC2 inhibits the amiloride-sensitive current and migration of glioma cells. *J Biol Chem* 281: 19220–19232, 2006.
44. **Wakui H, Tamura K, Tanaka Y, Matsuda M, Bai Y, Dejima T, Masuda S, Shigenaga A, Maeda A, Mogi M, Ichihara N, Kobayashi Y, Hirawa N, Ishigami T, Toya Y, Yabana M, Horiuchi M, Minamisawa S, Umemura S.** Cardiac-specific activation of angiotensin II type 1 receptor-associated protein completely suppresses cardiac hypertrophy in chronic angiotensin II-infused mice. *Hypertension* 55: 1157–1164, 2010.
45. **Wesseling S, Ishola DA Jr, Joles JA, Bluyssen HA, Koomans HA, Braam B.** Resistance to oxidative stress by chronic infusion of angiotensin II in mouse kidney is not mediated by the AT_2 receptor. *Am J Physiol Renal Physiol* 288: F1191–F1200, 2005.
46. **Wolak T, Kim H, Ren Y, Kim J, Vaziri ND, Nicholas SB.** Osteopontin modulates angiotensin II-induced inflammation, oxidative stress, and fibrosis of the kidney. *Kidney Int* 76: 32–43, 2009.
47. **Ye M, Wysocki J, William J, Soler MJ, Cokic I, Batlle D.** Glomerular localization and expression of angiotensin-converting enzyme 2 and Angiotensin-converting enzyme: implications for albuminuria in diabetes. *J Am Soc Nephrol* 17: 3067–3075, 2006.
48. **Zhai P, Yamamoto M, Galeotti J, Liu J, Masurekar M, Thaisz J, Irie K, Holle E, Yu X, Kupershmidt S, Roden DM, Wagner T, Yatani A, Vatner DE, Vatner SF, Sadoshima J.** Cardiac-specific overexpression of AT1 receptor mutant lacking G alpha q/G alpha i coupling causes hypertrophy and bradycardia in transgenic mice. *J Clin Invest* 115: 3045–3056, 2005.
49. **Zhuo JL, Imig JD, Hammond TG, Orengo S, Benes E, Navar LG.** Ang II accumulation in rat renal endosomes during Ang II-induced hypertension: role of AT_1 receptor. *Hypertension* 39: 116–121, 2002.
50. **Zou LX, Imig JD, von Thun AM, Hymel A, Ono H, Navar LG.** Receptor-mediated intrarenal angiotensin II augmentation in angiotensin II-infused rats. *Hypertension* 28: 669–677, 1996.

Journal of Molecular and Cellular Cardiology 50 (2011) 337–345

Contents lists available at ScienceDirect

Journal of Molecular and Cellular Cardiology

journal homepage: www.elsevier.com/locate/yjmcc

Original article

Cardiac origin of smooth muscle cells in the inflow tract

Haruko Nakano [a,b,1], Estrelania Williams [a,b,2], Masahiko Hoshijima [c,3], Mika Sasaki [d,e,2], Susumu Minamisawa [f,3], Kenneth R. Chien [d,e,*,4], Atsushi Nakano [a,b,*,5]

[a] Department of Molecular Cell and Developmental Biology, University of California, Los Angeles, Los Angeles, CA 90095, USA
[b] Eli and Edythe Broad Center of Regenerative Medicine and Stem Cell Research, University of California, Los Angeles, Los Angeles, CA 90095, USA
[c] Department of Medicine, Center for Research in Biological Systems, University of California, San Diego, La Jolla, CA 92093, USA
[d] Cardiovascular Research Center, Massachusetts General Hospital, Boston, MA 02114, USA
[e] Department of Stem Cell and Regenerative Biology, Harvard University, and the Harvard Stem Cell Institute, Cambridge, MA 02114, USA
[f] Department of Science and Engineering, Waseda University, Tokyo 169-8555, Japan

ARTICLE INFO

Article history:
Received 12 August 2010
Received in revised form 14 September 2010
Accepted 12 October 2010
Available online 23 October 2010

Keywords:
Cardiogenesis
Myogenic progenitor
Smooth muscle
Great vessel
Plasticity

ABSTRACT

Multipotent Isl1$^+$ heart progenitors give rise to three major cardiovascular cell types: cardiac, smooth muscle, and endothelial cells, and play a pivotal role in lineage diversification during cardiogenesis. A critical question is pinpointing when this cardiac–vascular lineage decision is made, and how this plasticity serves to coordinate cardiac chamber and vessel growth. The posterior domain of the Isl1-positive second heart field contributes to the SLN-positive atrial myocardium and myocardial sleeves in the cardiac inflow tract, where myocardial and vascular smooth muscle layers form anatomical and functional continuity. Herein, using a new atrial specific SLN-Cre knockin mouse line, we report that bipotent Isl1$^+$/SLN$^+$ transient cell population contributes to cardiac as well as smooth muscle cells at the heart-vessel junction in cardiac inflow tract. The Isl1$^+$/SLN$^+$ cells are capable of giving rise to cardiac and smooth muscle cells until late gestational stages. These data suggest that the cardiac and smooth muscle cells in the cardiac inflow tract share a common developmental origin. This article is part of a special issue entitled, "Cardiovascular Stem Cells Revisited".

1. Introduction

The cardiac, smooth muscle and endothelial cells arise from single, common multipotent precursor cells during embryogenesis [1–3]. Whereas three major cardiovascular lineages can arise from Flk1$^+$/Bry$^+$ mesodermal progenitors [1,4] and Flk1$^+$/Isl1$^+$/Nkx2.5$^+$ cardiogenic colonies derived from mouse embryos around E8.0–8.5 [2], smooth muscle cell lineages can also arise from c-kit$^+$/Nkx2.5$^+$ cardiac progenitor cells isolated from a later stage [3]. These progenitor populations may represent discrete lineages that constitute the heart [5]. Alternatively, they may represent cells in the same lineage at different developmental stages. The comparison of these analyses suggests that the endothelial lineage separates from the myogenic lineage at an early stage, whereas cardiac and smooth muscle lineages are closely related until later stages of cardiogenesis [6,7]. Given that the plasticity of progenitors becomes progressively restricted as embryogenesis proceeds, intriguing questions are which population displays cardiac-smooth muscle bipotency, how long the progenitors maintain their plasticity during cardiogenesis and what is the biological implication of smooth muscle differentiation capability of the cardiac progenitors.

The second heart field (SHF) is delineated by the expression of Isl1, a member of the LIM-homeodomain transcription factor family. This extra-crescent cardiac population is specified in the anterior lateral plate mesoderm adjacent to the first heart field (FHF) in the cardiac crescent [7–9]. After the FHF forms a single straight primitive heart tube, the SHF progenitors migrate from the splanchnic mesoderm towards the primitive heart tube and trigger its right-ward looping. These SHF progenitors continue to migrate and add additional myocardium to the primitive heart tube until midgestational stages. The SHF progenitors downregulate Isl1 expression immediately after completing their migration, which makes Isl1 a suitable marker of an immature state for cardiac progenitors. During this step, the Isl1$^+$ cardiac progenitors in the anterior region of the SHF (aSHF, also known as anterior heart field; AHF) migrate to the arterial pole of the heart tube and form the outflow tract and right ventricle [10–12]. This anterior subpopulation is distinguishable from other subpopulations of Isl1-positive SHF progenitors by several molecular markers

* Corresponding authors. K.R. Chien is to be contacted at Cardiovascular Research Center, Massachusetts General Hospital, Boston, MA 02114, USA. A. Nakano, Department of Molecular Cell and Developmental Biology, University of California, Los Angeles, Los Angeles, CA 90095, USA. Tel.: +1 310 267 1897.
E-mail addresses: kchien@partners.org (K.R. Chien), anakano@ucla.edu (A. Nakano)

[1] Conception and design, collection and/or assembly of data, data analysis and interpretation, manuscript writing.
[2] Collection and/or assembly of data.
[3] Conception and design, data analysis and interpretation.
[4] Conception and design, data analysis and interpretation, manuscript writing.
[5] Conception and design, collection and/or assembly of data, data analysis and interpretation, manuscript writing.

0022-2828/$ – see front matter © 2010 Elsevier Ltd. All rights reserved.
doi:10.1016/j.yjmcc.2010.10.009

including specific enhancers of Mef2c [13] and FGF10 [10], suggesting that Isl1-positive cells are already heterogeneous at this stage. The $Isl1^+$ progenitors in the aSHF eventually acquire a ventricular phenotype and contribute to the myocardium of the outflow tract and the right ventricle. Interestingly, this population also developmentally gives rise to smooth muscle cells in the root of the aorta [14]. On the other hand, Isl1-positive progenitors in posterior part of the SHF (pSHF) populate the venous pole of the primary heart tube slightly later, maintain high proliferative and migratory activity, and express Isl1 until midgestational stages [15,16]. This posterior subpopulation of late Isl1-positive progenitors eventually acquires an atrial phenotype and contributes to the myocardium in atrial chambers and myocardial sleeves in the inflow tract. Thus, at the linear heart tube stage, the $Isl1^+$ cardiac progenitor population seems to be a pool of several different subsets of cardiac progenitors including aSHF and pSHF populations. Whereas Isl1-positive progenitors in the outflow tract/arterial pole/aSHF are known to give rise to both cardiac and smooth muscle cells, it is not clear if myocardium and smooth muscle in the inflow tract share a common cellular origin in the venous pole/pSHF. This is in part because of the lack of a specific lineage marker and in part because of the lack of single cell analysis.

Sarcolipin (SLN) is an inhibitor of sarco(endo)plasmic reticulum Ca^{2+}-ATPase (SERCA) that is specifically expressed in atrial myocardium and skeletal muscle, and implicated in atrial specific contractile function [17–19]. SLN expression is gradually upregulated as the atrial myocytes maturate, and is a useful marker for the atrial muscle lineage.

Here, we report the generation of atrial specific SLN-Cre knockin mouse line, and the identification of $Isl1^+/SLN^+$ cells in the atrial lineage which contribute to atrial cardiomyocytes and smooth muscle cells in the cardiac inflow tract. To investigate the differentiation capability of $Isl1^+/SLN^+$ cells, we generated an atrial specific deleter mouse line by introducing Cre recombinase into the SLN locus. SLN-labeled atrial cells distribute in working and SA nodal atrial myocytes, as well as the smooth muscle cells in the cardiac inflow tract. *In vitro* assays indicate that $Isl1^+/SLN^+$ cells are capable of clonally differentiating into cardiomyocytes and smooth muscle cells from single progenitors. Interestingly, $Isl1^+/SLN^+$ cells retain smooth muscle competency until late gestational stages. These observations provide an insight into the origin of cardiac and smooth muscle cells at the boundary of the atrial chamber and inflow tract, and the mechanism underlying the formation of heart-vessel junctions.

2. Materials and methods

2.1. Generation of SLN-Cre mice

Exon 2 of the *SLN* locus including the 1st ATG was replaced with Cre cDNA. A correctly targeted R1 ES clone was screened by Southern blotting and genomic PCR. The recombination efficiency was 1/300 clones.

2.2. Preparation of cardiac mesenchymal feeder layer

Neonatal hearts were predigested with 0.5 mg/ml trypsin in HBSS at 4 °C overnight followed by strong digestion with collagenase at 37 °C for 1 h (0.5 mg/ml in HBSS). Cardiac mesenchymal fibroblasts were separated from myocytes by differential plating for 1 h twice. Fibroblasts from the first and the second differential plating were combined, grown until confluent and treated with 10 μg/ml mitomycin C for 2 h on the day before progenitors were seeded. The contamination of myocytes in the fibroblast fraction was less than 0.07% by cTnT staining.

2.3. Histology and immunostaining

Whole mount and section Xgal stainings were performed according to standard protocols. Double staining for Xgal and specific antibodies were performed as follows: 8 μm frozen sections or cells were stained with Xgal followed by postfixation for 5 min, 0.3% hydrogen peroxide treatment for 15 min, blocking with 10% normal goat serum for 1 h and antibody reaction in 3% normal goat serum at 4 °C overnight. Secondary antibody reaction was performed with Vectastain ABC kit (Vector lab) according to the manufacturer's protocol. Section Xgal/Isl1 staining was performed as previously described [20]. The concentrations of the primary antibodies are as follows: cTnT (1:200, Lab Vision Corp., Fremont, CA), smMHC (1:500, Biomedical Technologies Inc., Stoughton, MA), Isl1 (1:200, DSHB, Iowa City, IA), and DsRed (1:500, Clontech, Mountain View, CA).

2.4. RT-PCR and qPCR

RNA was extracted with Trizol (Invitrogen, Carlsbad, CA) or Absolute nanoprep kit (Stratagene, Ceder Creek, TX) according to the manufacturer's protocol, and cDNAs were synthesized with iScript kit (BioRad, Hercules, CA). Colony PCR was run for 35 cycles. Quantitative PCR was performed with the SYBR Green system and i-Cycler (BioRad, Hercules, CA).

2.5. Electron microscopic analysis

The $SLN^{cre/+}$; *R26R* hearts were dissected and fixed in 1% PFA and 2.5% glutaraldehyde in PBS for 3 h, and stained for 4 h in Bluo-gal staining solution; 1 mg/ml Bluo-gal (Sigma), 10 mM ferro/ferri cyanide, 2 mM MgCl2, 0.02% NP40 and 0.01% NaDOC. Stained tissues were post-fixed for 30 min in a mixture of 1% osmium tetroxide and 2% glutaraldehyde in 0.15 M cacodylate buffer (on ice), washed several times in PBS, and dehydrated in graded ethanol and acetone (all steps on ice). Preparations were left overnight in a 1:1 mixture of Epon and acetone and then for 5–10 h in unpolymerized Epon. They were transferred to molds, oriented and placed at 60 °C for 24 h to permit polymerization of the Epon. Sections were mounted on net grids (Ted Pella) and treated with uranyl acetate and lead citrate.

3. Results

3.1. SLN-Cre knockin strain is a sensitive and specific deleter line for the atrial lineage

To generate an atrial specific Cre line driven by an internal promoter, we introduced Cre recombinase by homologous recombination into exon 2 of the *SLN* locus (Figs. 1A, B, C). $SLN^{cre/+}$ heterozygotes displayed no morphological or fertility defects. While SLN mRNA is expressed at E10.0 (Fig. 2A), the βgal activity in $SLN^{cre/+}$; *R26R* embryos was first detected in the atria at around E10.5, when Isl1 is still positive in the atrial lineage (Fig. 2B). After E12.5, the atrial myocardium was broadly and strongly labeled by R26R and CAG-DsRed reporter lines [21,22] (Figs. 2C–H″, and S1A, B). Section Xgal staining of the neonatal hearts revealed that the vast majority of the atrial myocytes were labeled (Figs. 2E, F), whereas none of the endocardial or epicardial cells were stained (Fig. 2F, arrowheads; Supplemental Table 1). Interestingly, HCN4-positive SA nodal cells were also labeled by SLN-Cre (Fig. S2). These data suggest that the SLN-Cre line is a sensitive and specific deleter line for the atrial lineage. To our knowledge, this mouse is the first deleter line in which Cre recombinase is driven by an internal atrial specific promoter.

Xgal staining in the inflow region visualized the anatomical distribution of the myocardial sleeves of the venae cavae and pulmonary veins. The Xgal staining extended up to bifurcation of the internal jugular and subclavian veins in the cranial region, and

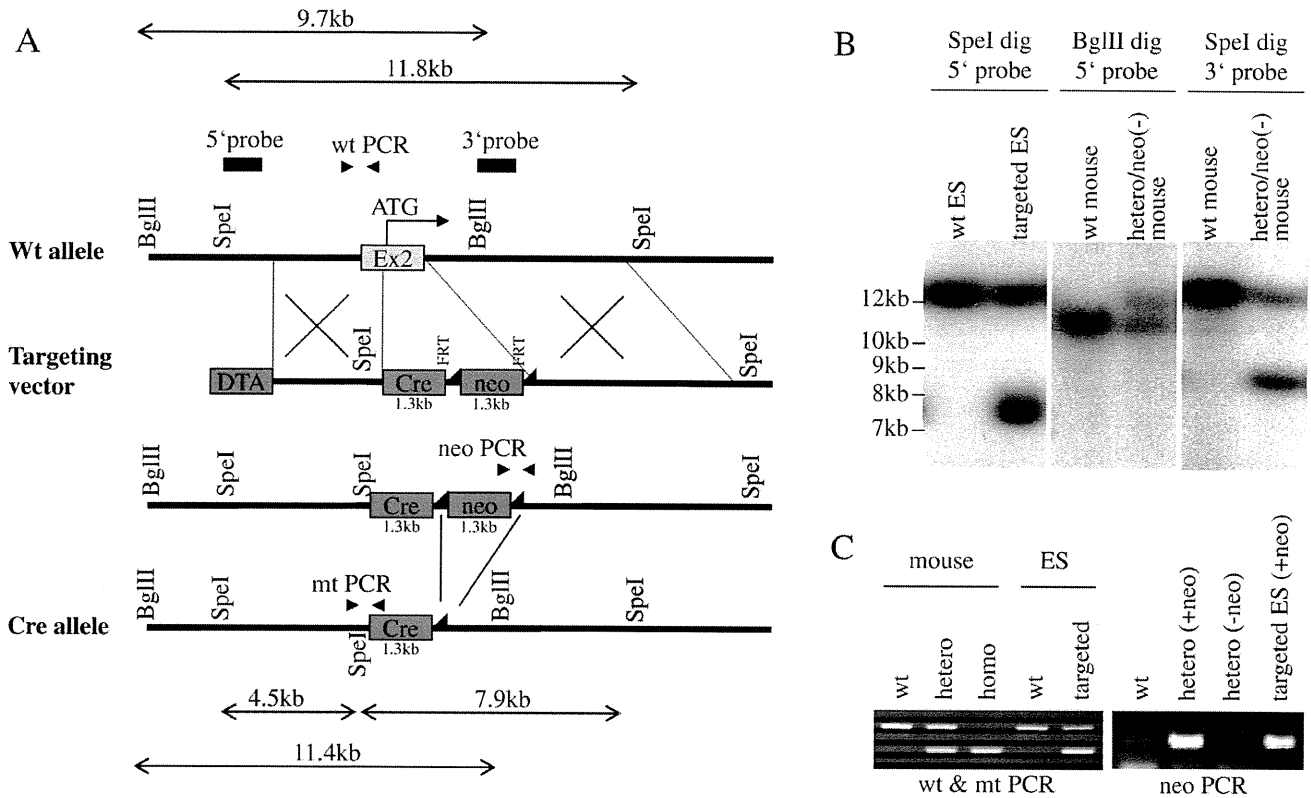

Fig. 1. Generation of SLN-Cre knockin mouse line. (A) Schematic of *SLN* genomic locus, targeting vector design and recombinant alleles. Exon 2 which includes the start codon was replaced by Cre recombinase and neomycin resistant cassette by homologous recombination. FRT sites are indicated by filled triangles. DTA, diphtheria toxin A cassette. (B) Genomic Southern blot analysis of targeted ES cells and heterozygous mouse after removal of neo cassette using 5′ and 3′ probes shown in A. (C) Genomic PCR for mouse genotyping. Primer designs are shown in A.

down to the diaphragm in the thoracic cavity (Figs. 2I–K and S1C). The boundary of the right atrium and the venae cavae is demarcated by venous valves that also are derived from *SLN*-expressing cells (Fig. 3A, arrowhead). Whereas the muscular layer of the atrial chamber consists only of myocardial cells, the muscular wall of the venae cavae distal to the venous valves consist of two muscular layers—the outer myocardial layer derived from SLN-expressing cells and inner smooth muscle layer positive for smMHC, a definitive marker for vascular smooth muscle cells (Fig. 3A). The myocardial layer tapers off towards the periphery and generates myocardial sleeves in the great veins. Similar to the vena cavae, the proximal region of the pulmonary veins also showed a two-layer structure with outer myocardial sleeve and inner smooth muscle layer (Fig. S3).

3.2. SLN-positive cells give rise to smooth muscle cells in cardiac inflow tract

Further analysis of this two-layer structure revealed the close relationship between cardiac and smooth muscle lineages during cardiovascular development. Double staining of serial sections showed that about 5–10% of smMHC-positive cells in the inflow region are co-stained with Xgal (Figs. 3C, D, black arrows; Supplemental Table 1). To confirm this, the inflow region of the atrium from $SLN^{cre/+}$; *R26R* adult mice was enzymatically dissociated and cultured on a fibronectin-coated dish. Consistent with section stainings, a fraction of βgal-labeled cells were co-stained for smMHC (Fig. 3B). Furthermore, electron microscopic analysis of Bluo-gal-stained $SLN^{cre/+}$; *R26R* hearts revealed that the smooth muscle cells with non-striated myofilaments are labeled with Bluo-gal deposits on their membranes (Figs. 3E, E′, arrowheads). βGal-labeled smooth muscle cells were also found in myocardial sleeves in the pulmonary veins (Fig. S3). These data suggest the developmental contribution of SLN-positive cells to the smooth muscle cells in the cardiac inflow tract. It has been reported that *SLN* mRNA is expressed strongly in atria and esophageal muscle and least abundantly in skeletal muscle and bladder, but no expression has been detected in vascular smooth muscle [18]. Consistently, our SLN-Cre lineage tracing experiments fail to detect any Xgal-positive smooth muscle cells in aortic or other major vasculature. Therefore, our findings raise the possibility that these two different cell types in the cardiac inflow region share a common cellular origin during cardiogenesis.

3.3. $Isl1^{+}/SLN^{+}$ cells represent a transient cell population in the venous pole

To examine the cellular origin of cardiac and smooth muscle cells in the inflow tract, we searched for Isl1-positive cells in the atrial lineage. As *in situ* hybridization and lineage tracing experiments indicated that SLN is expressed from E10.0 and on in the atria (Fig. 2A), and Isl1 expression continues until midgestation [15], we speculated that there is a spatial and temporal overlap of these two markers in the forming atria. Double staining for Xgal and Isl1 on $SLN^{cre/+} \times R26R$ embryos revealed Isl1/SLN double positive cells in forming atria (Fig. 4). At E10.5, immature cardiac progenitors with strong Isl1 expression were found in the splanchnic mesoderm (Fig. 4A, arrowheads). Cells in the primary atrial septum are also positive for Isl1 (Fig. 4A, white arrow). A subset of